The Abdus Salam
International Centre for Theoretical Physics

United Nations
Educational, Scientific and
Cultural Organization

IAEA
International Atomic Energy Agency

2141-18

Joint ICTP-IAEA Workshop on Nuclear Reaction Data for Advanced Reactor Technologies

3 - 14 May 2010

A Very Brief Overview of Reaction Theory

CARLSON B.V.
ITA-CTA, Sao Jose dos Campos
Sao Paulo
BRAZIL

A Very Brief Overview

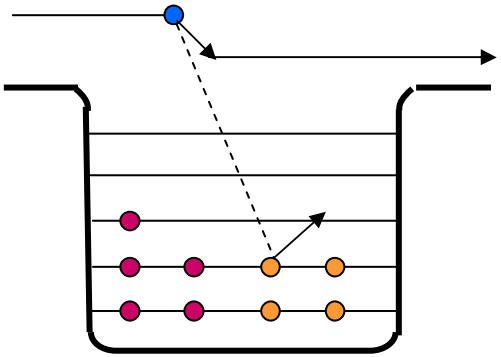

# of Reaction Theory

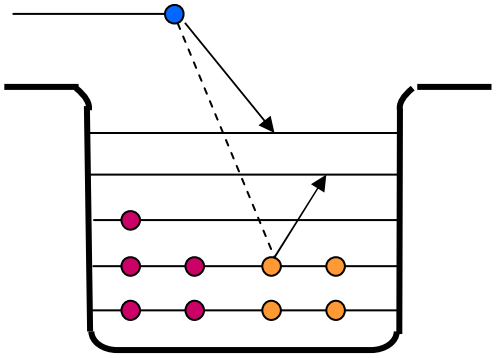

B.V. Carlson -- Depto. de Física
Instituto Tecnológico de Aeronáutica
São José dos Campos SP, Brazil

Nuclear Scattering and Reactions

- Elastic scattering – (n, n), (p, p), (α ,α), ...
- Inelastic Scattering -- (n, n′), (p, p′), (α ,α'), ...
- Knockout/emission – (n, 2n), (n, np), (p, pn), (p, 2p), ...
- Stripping – (d, p), (d, n), (t, d), ...
- Pickup – (p, d), (n, d), (d, t), ...
- Charge exchange – (n,p), (p,n), (t,^{3}He), (^{3}He, t), ...
- Fission – (n,f), (p,f), (α,f), ...

Depending on the incident energy and the combination of projectile and target, some or many of these reactions can occur in a nuclear collision.

We will find that they often occur through two very different mechanisms – a fast, direct one and a slower, composite nucleus one.

Conservation laws

Conservation laws are important in determining the basic characteristics of nuclear reactions.

- Charge and nucleon number, Z and A -- ^{56}Fe (p, n) ^{56}Co
- Energy, E – ^{238}U(n,n′)^{238}U* (E_x= 0.045 MeV)
- Linear momentum, $\vec{p}$ – thresholds, recoil
- Angular momentum and parity, $\vec{J}$ and π -- $d\sigma/d\Omega$

Parity is not conserved in weak interactions, e.g. in β decay and electron conversion, but we will not consider these processes here.

Experimental Setup for Studying Scattering

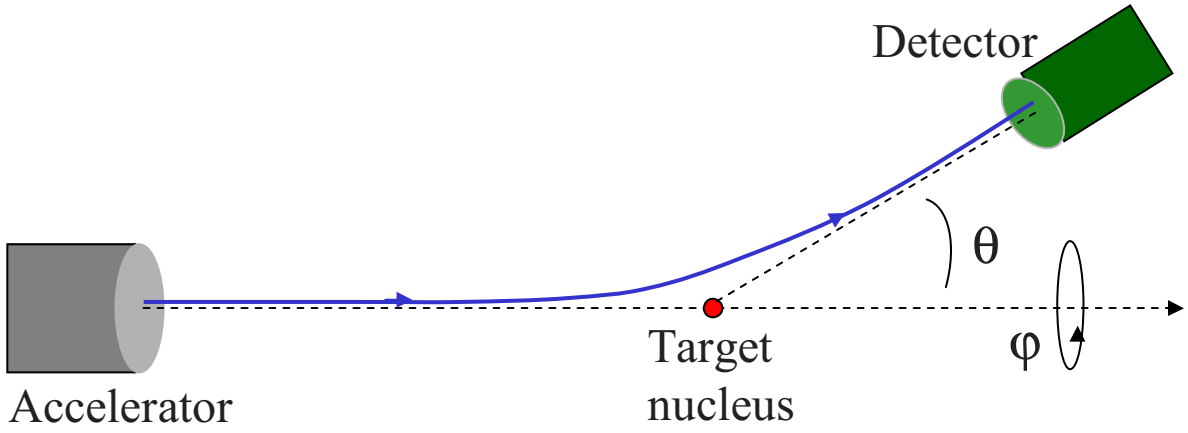

•Distance from accelerator to target and from target to detector on the order of a meter or more.

•Cross sectional area of beam A on the order of mm^2.

•Target thickness t on the order of μm or more.

•Beam intensity – n_0 (particles/s) – varies greatly, from about 10^5 to 10^{13}

•In target, atomic dimension on the order of 10^{-10} m and nuclear dimension on the order of 10^{-15} m.

The Experimental Cross Section

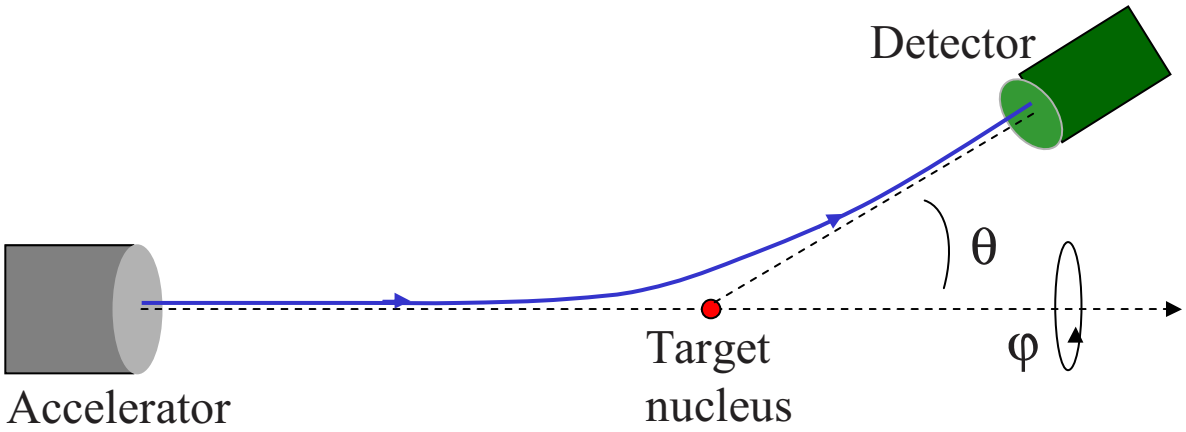

- A – cross sectional area of beam
- ρ_{tar} – target particle density
- n_0 – incident beam intensity
- t – target thickness
- $n(\theta,\varphi)d\Omega$ -- particle intensity (part./s) entering detector of solid angle $d\Omega$

$$d\sigma = \frac{\text{particle intensity entering detector in solid angle } d\Omega}{\text{(incident intensity/area) * (no. of target particles in beam)}} = \frac{n(\theta,\varphi)\,d\Omega}{\left(n_0 / A\right)\left(\rho_{tar}\,tA\right)}$$

The differential cross section $\dfrac{d\sigma}{d\Omega}$ has the units of area/solid angle.

The Classical Cross Section

b – the impact parameter

- perpendicular distance between particle trajectory and center of target

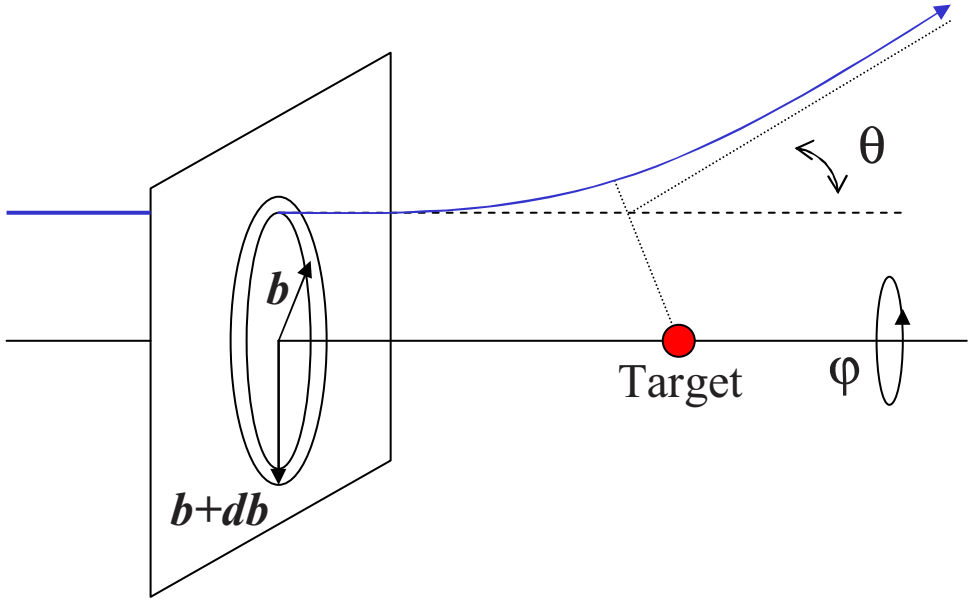

Assuming no dependence on φ,

$$\frac{d\sigma}{d\theta} = 2\pi\, b(\theta)\left|\frac{db}{d\theta}\right|$$

Since

$$d\Omega = 2\pi \sin\theta\, d\theta$$

$$\Rightarrow \quad \frac{d\sigma}{d\Omega} = \frac{b(\theta)}{\sin\theta}\left|\frac{db}{d\theta}\right|$$

An example – Hard sphere scattering

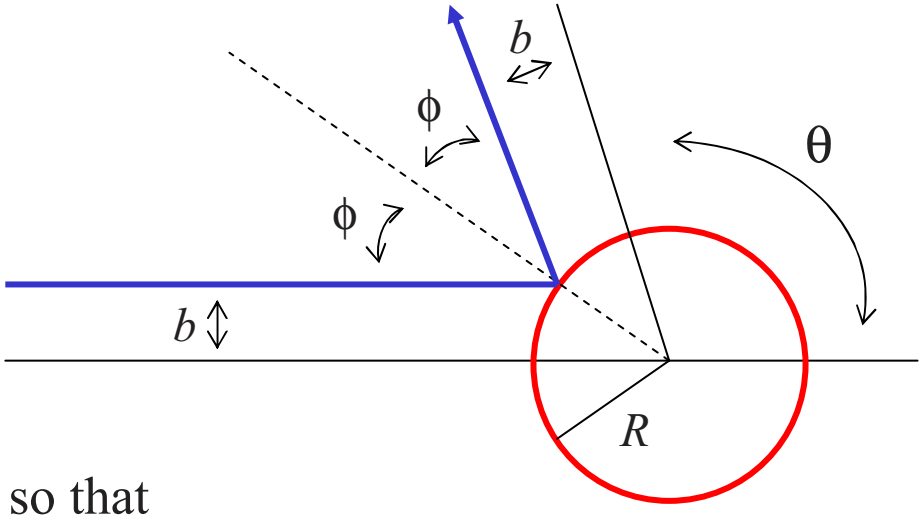

We have

$$b(\phi) = R\sin\phi$$

and

$$\phi = \frac{\pi - \theta}{2}.$$

so that

$$\frac{d\sigma}{d\theta} = 2\pi\, b(\theta)\left|\frac{db}{d\theta}\right| = \frac{\pi R^2}{2}\sin\theta$$

and

$$\frac{d\sigma}{d\Omega} = \frac{b(\theta)}{\sin\theta}\left|\frac{db}{d\theta}\right| = \frac{R^2}{4}$$

For ^{238}U, R ≈ 7.5 fm and

$R^2/4 \approx 14$ fm^2 = 140 mb.

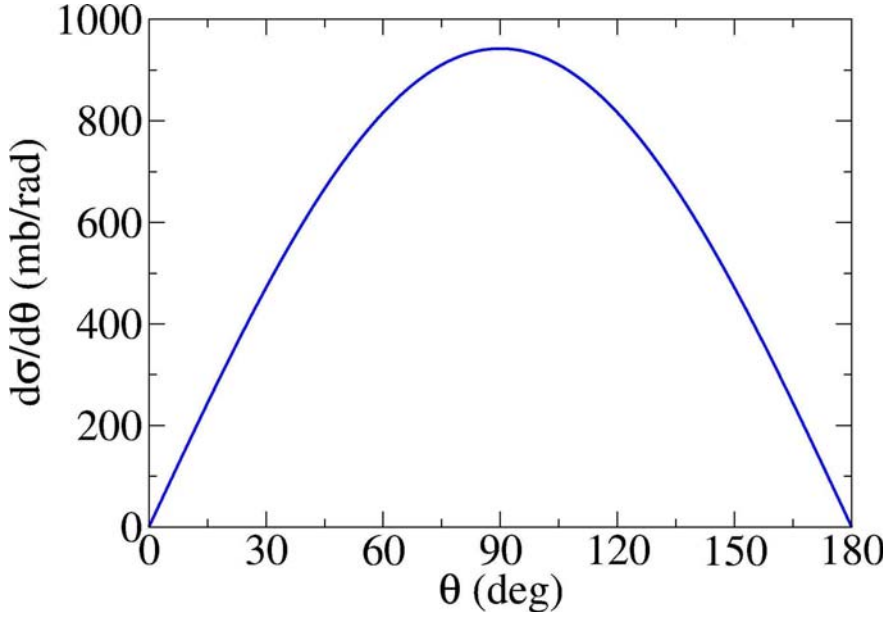

Another example – a sticky hard sphere

Now, suppose that a fraction of the incoming particles do not scatter, but instead stick to the target. Let us assume, for instance, that the fraction

$$P(\theta) = \alpha \cos\phi = \alpha \sin\frac{\theta}{2}$$

(which decreases as the collision becomes more grazing) is absorbed by the target.

Decomposition of the differential cross section:

$$\frac{d\sigma_{abs}}{d\theta} = \frac{\pi R^2}{2} P(\theta) \sin\theta$$

$$\frac{d\sigma_{el}}{d\theta} = \frac{\pi R^2}{2} (1 - P(\theta)) \sin\theta$$

$$\frac{d\sigma_{tot}}{d\theta} = \frac{d\sigma_{abs}}{d\theta} + \frac{d\sigma_{el}}{d\theta} = \frac{\pi R^2}{2} \sin\theta$$

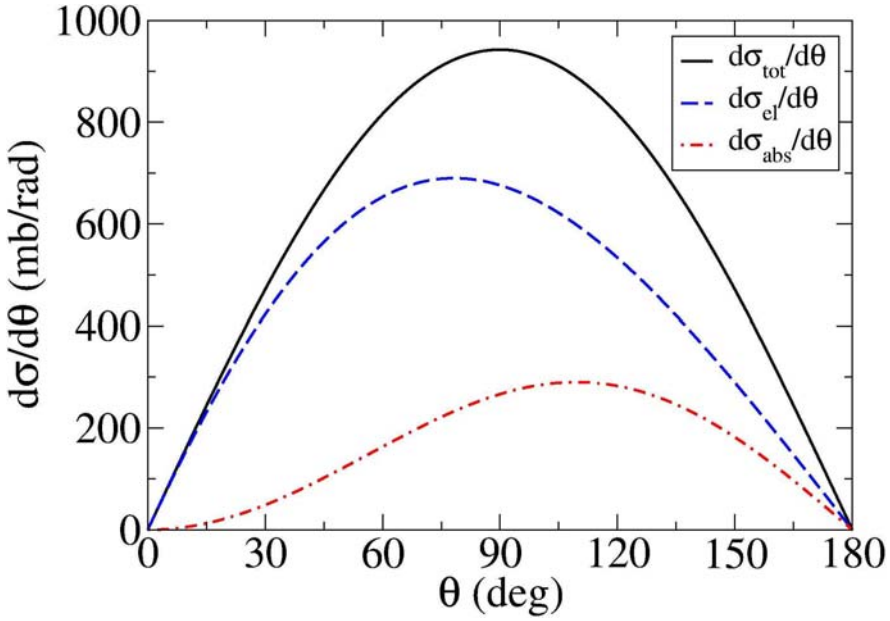

Only $d\sigma_{el}/d\theta$ is observed as scattered particles. In the figure, $\alpha = 0.4$

Integrated cross sections

We can integrate the differential cross sections over angle to obtain

$$\sigma_{abs} = \frac{\pi R^2}{2}\int_0^{\pi} P(\theta)\sin\theta\, d\theta = \frac{2}{3}\alpha\pi R^2$$

$$\sigma_{el} = \frac{\pi R^2}{2}\int_0^{\pi} \left(1-P(\theta)\right)\sin\theta\, d\theta = \left(1-\frac{2}{3}\alpha\right)\pi R^2$$

$$\sigma_{tot} = \sigma_{abs} + \sigma_{el} = \pi R^2$$

The total cross section of πR^2 is what we would expect and what we would obtain in the simple hard sphere case.

In the general case, when there is a value of the impact parameter b_{max} such that $\theta(b)=0$ for $b>b_{max}$, we have

$$\sigma_{tot} = 2\pi\int_0^{\pi} b(\theta)\left|\frac{db}{d\theta}\right| d\theta = \pi b^2\Big|_0^{b_{\max}} = \pi b_{\max}^2$$

Attenuation and the total cross section

Both elastic scattering and absorption remove particles from the incident beam. The sum of the two – the total cross section – determines how the beam is attenuated as it passes through the target.

From the definition of the cross section, we have in any dz

$$\sigma_{tot} = \frac{-dn}{n(z)\,\rho_{tar}\,dz}$$

or

$$\frac{dn}{dz} = -\rho_{tar}\,\sigma_{tot}\,n(z)$$

$$\Rightarrow \quad n(z) = n_0 \exp\left(-\rho_{tar}\sigma_{tot}\,z\right)$$

The inverse of the product $\rho_{tar}\sigma_{tot}$ defines the mean free path λ of the projectile through the target.

$$\lambda = 1/\rho_{tar}\sigma_{tot}$$

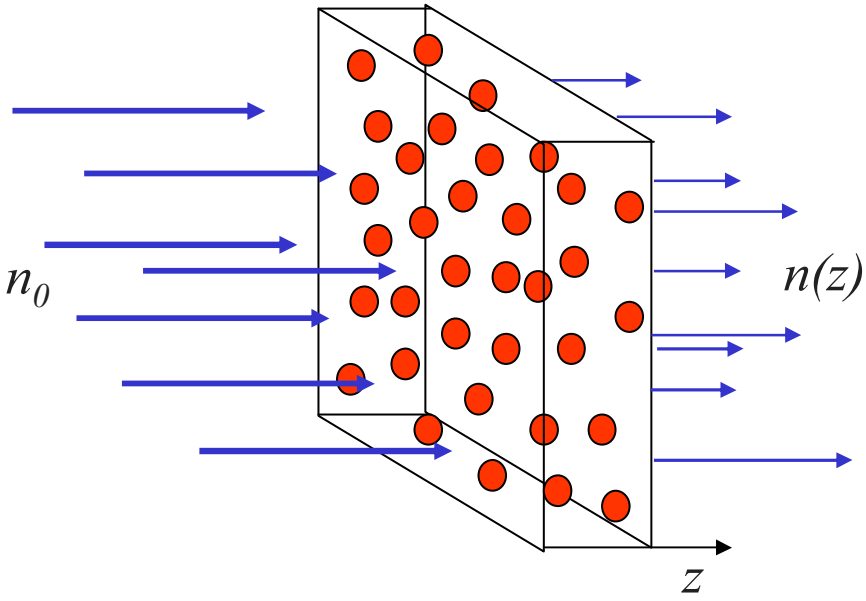

For our example of hard scattering from U-like spheres, assuming a density close to that of U, we have

$$\lambda = \left(\frac{19*6}{238}\times 10^{29} * 177\times 10^{-30}\ \mathrm{m}^{-1}\right)^{-1} \approx 0.12\,\mathrm{m}$$

Laboratory and Center-of-mass Coordinates

In order to properly treat the conservation of momentum and energy, scattering problems should be analyzed in the center-of-mass frame.

The basic steps in the transformation to the center-of-mass frame and back to the lab one are shown below.

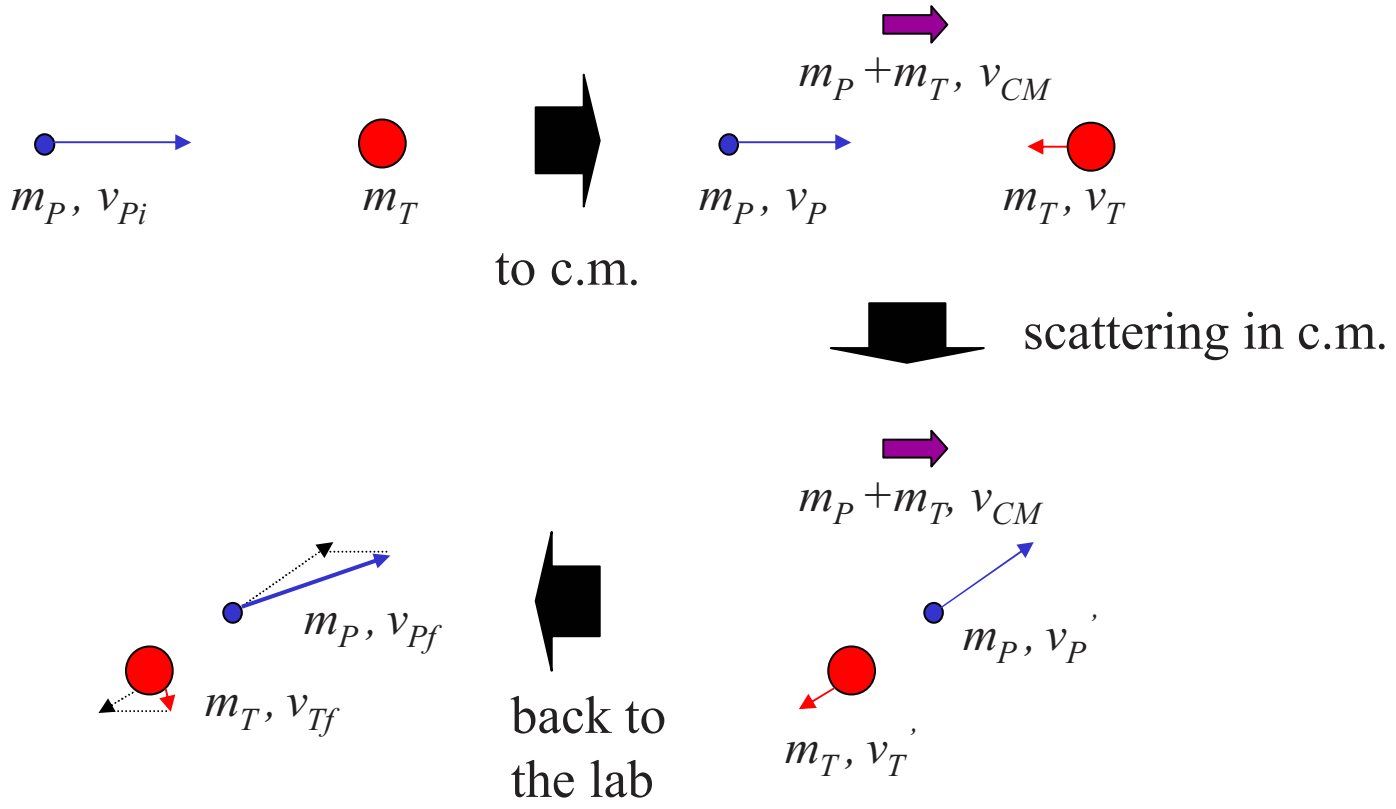

Laboratory and Center-of-mass Coordinates - Basics

Two fundamental quantities that result from the transformation are the reduced mass μ and the energy E_{cm} in the center-of-mass frame. In terms of the projectile and target masses, m_P and m_T and the projectile energy in the lab frame E_{lab}, these are

$$\mu = \frac{m_P m_T}{m_P + m_T} \qquad \text{and} \qquad E_{cm} = \frac{m_T}{m_P + m_T} E_{lab}$$

The relative velocity in the c.m. frame is the same as that in the lab frame,

$$v_{cm,rel} = v_{lab,rel}$$

The transformation of the scattering angle does not reduce to a simple expression. However, its numerical calculation is straightforward.

From this point on, we will assume that we are using the center-of-mass frame, unless otherwise noted.

Waves and particles

We know that the wave-like nature of the scattering particles may be neglected only if their wavelength is much smaller than the length scale on which the scattering system varies. For nuclear scattering, the appropriate length scale would be at most the size of the nucleus and should probably be of the size of the nuclear surface – about 0.5 to 1.0 fm.

Comparing the wavelength of a nucleon to a typical nuclear radius, taken to be $R = 1.25A^{1/3}$ (fm), we find that the wavelike nature must be taken into account over the entire energy range we will consider – up to about 20 MeV.

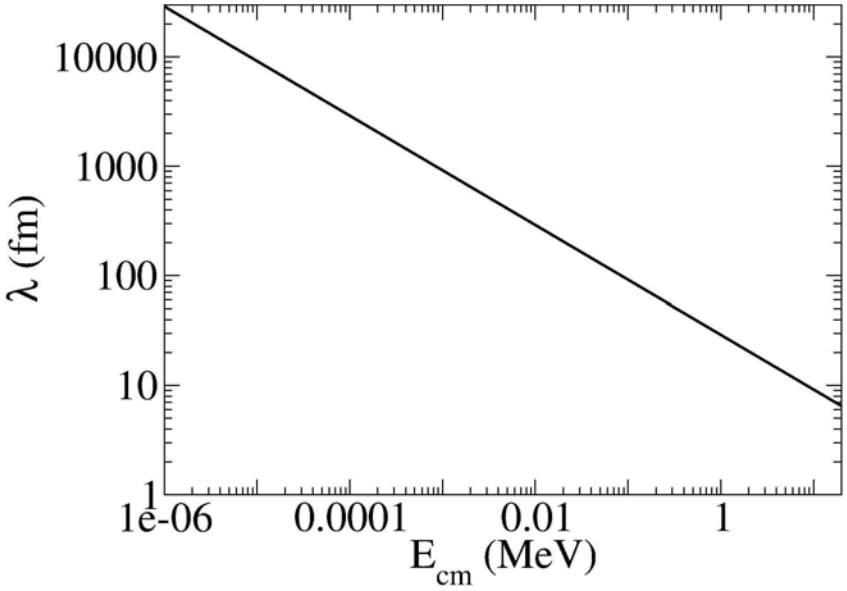

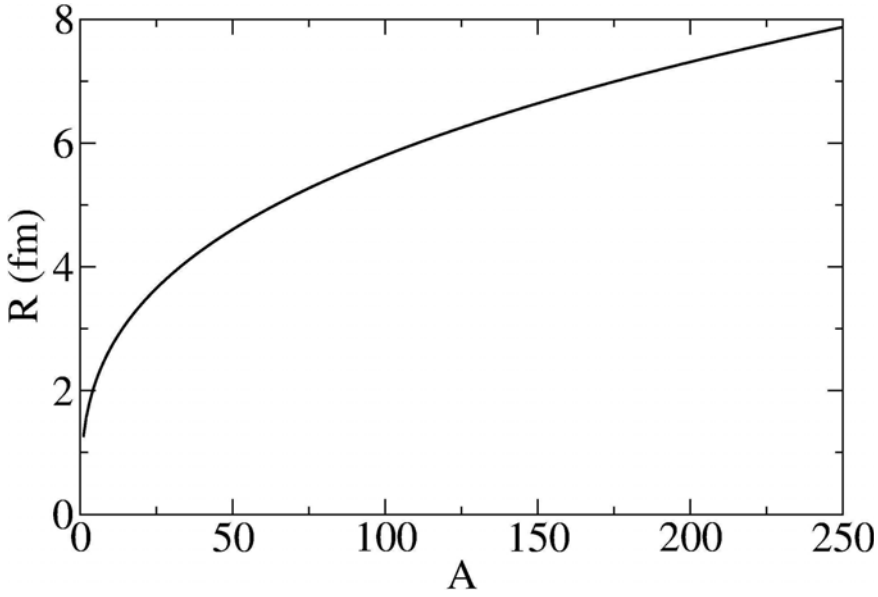

The quantum view of scattering

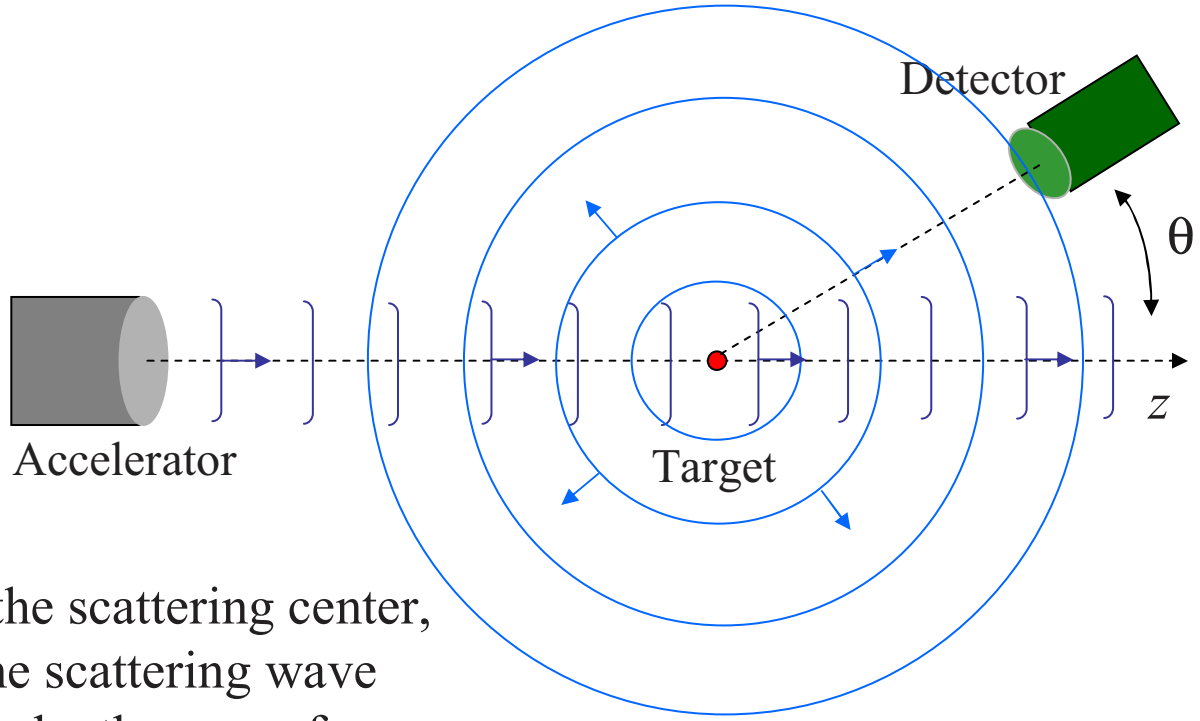

Far from the scattering center, we take the scattering wave function to be the sum of a plane wave and a scattered outgoing spherical wave,

$$\psi(\vec{r}) \to e^{ikz} + f(\theta)\frac{e^{ikr}}{r}.$$

when $r \to \infty$. $\left(k^2 = 2\mu E_{cm}/\hbar^2\right)$

The differential cross section is the squared magnitude of the scattering amplitude,

$$\frac{d\sigma}{d\Omega} = \left|f(\theta)\right|^2.$$

The partial-wave expansion

Neglecting spin, we use conservation of angular momentum to expand the wave function in partial waves of the orbital angular momentum,

$$\psi(r,\theta) = \sum_{l=0}^{\infty} u_l(r) P_l(\cos\theta).$$

The plane wave may be expanded as

$$e^{ikz} = \sum_{l=0}^{\infty} (2l+1) i^l j_l(kr) P_l(\cos\theta)$$

with

$$j_l(kr) = \frac{i}{2}\left(h_l^{(-)}(kr) - h_l^{(+)}(kr)\right) \qquad \text{where} \qquad h_l^{(\pm)}(kr) \xrightarrow[r\to\infty]{} (\mp i)^l \frac{e^{\pm ikr}}{kr}.$$

In analogy with the plane wave, we write

$$\psi(r,\theta) \to \sum_{l=0}^{\infty} (2l+1) i^l \frac{i}{2}\left(h_l^{(-)}(kr) - S_l h_l^{(+)}(kr)\right) P_l(\cos\theta)$$

$$\to e^{ikz} + \frac{1}{2ik}\sum_{l=0}^{\infty} (2l+1)\left(S_l - 1\right) P_l(\cos\theta)\frac{e^{ikr}}{r},$$

when $r \to \infty$.

Cross sections

We obtain the elastic cross section by integrating over the differential one,

$$\sigma_{el} = 2\pi \int_0^{\pi} |f(\theta)|^2 \sin\theta d\theta = \frac{\pi}{k^2} \sum_{l=0}^{\infty} (2l+1) |S_l - 1|^2 .$$

We may calculate the absorption cross section by taking into account all of the flux entering and leaving the scattering region. Integrating the flux over a sphere whose radius tends to infinity, we have

$$\sigma_{abs} = -\frac{1}{v} \int_S \vec{j} \cdot d\vec{S} = \frac{\pi}{k^2} \sum_{l=0}^{\infty} (2l+1) \left(1 - |S_l|^2\right).$$

The total cross section takes into account all flux lost from the incident plane wave, either by scattering or absorption,

$$\sigma_{tot} = \sigma_{el} + \sigma_{abs} = \frac{2\pi}{k^2} \sum_{l=0}^{\infty} (2l+1) \left(1 - \mathrm{Re}\, S_l\right).$$

Low-energy neutron scattering – a simple example

Because of the Coulomb barrier, only neutral particles can reach the nucleus in a low-energy scattering. At extremely low energies, the centripetal barrier keeps all but l=0, s-waves away from the nucleus.

Let us examine hard-sphere scattering in the case of low-energy neutron scattering.

Scattering from the hard sphere requires that the wave-function vanish at the radius of the sphere. The s-wave wave function is then

$$\psi_0(r) = \frac{i}{2kr}(e^{-ikr} - e^{-2ikR}e^{ikr}).$$

The S-matrix element is $S_0 = e^{2ikR}$.

The elastic cross section is

$$\sigma_{el} = 4\pi\frac{d\sigma}{d\Omega} = \frac{\pi}{k^2}\left|e^{-2ikR} - 1\right|^2.$$

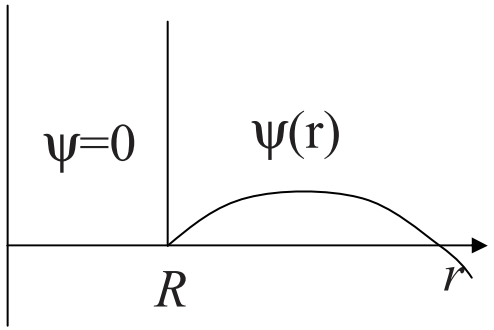

When $k \to 0$, the elastic cross section tends to a constant,

$$\sigma_{el} \xrightarrow[k\to 0]{} 4\pi R^2.$$

This is 4 times the classical cross section.

Low-energy neutron scattering -- resonances

Although the neutron-nucleus interaction is attractive, its rapid variation at the nuclear surface has the same effect on low energy neutrons as a hard-sphere does– the neutrons are reflected. Absorption also usually occurs, so that the total cross section is larger than the elastic one. However, if both the elastic scattering and absorption are prompt processes, one would expect them to vary slowly with energy. Behavior of this type can be seen on the low energy side of the figure.

The cross section of the figure also possesses a rapidly varying resonant component, a feature common to all low-energy neutron-nucleus systems.

The resonant contribution arises from scattering through a quasi-bound state (a compound nuclear state) of the neutron+nucleus.

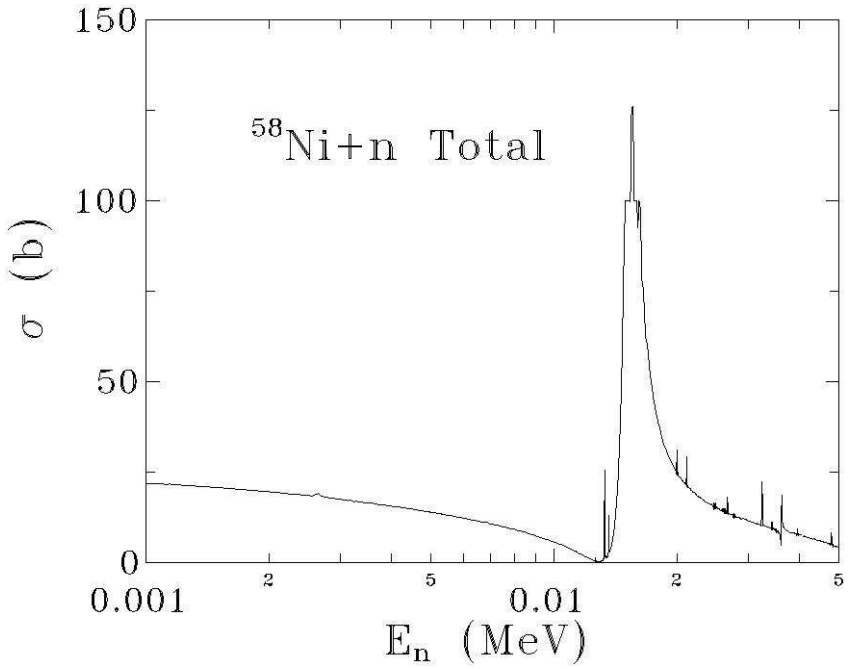

Direct and compound nuclear scattering

At low energies, neutron-nucleus scattering occurs either directly or through the quasi-bound compound nucleus states.

Direct scattering

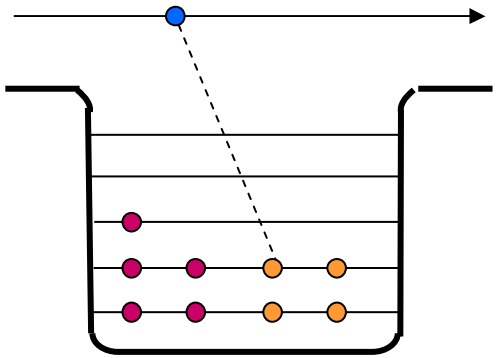

$\Delta t \sim 10^{-20} - 10^{-22}$ s

$\Delta E \Delta t \geq \hbar$

Compound nuclear scattering

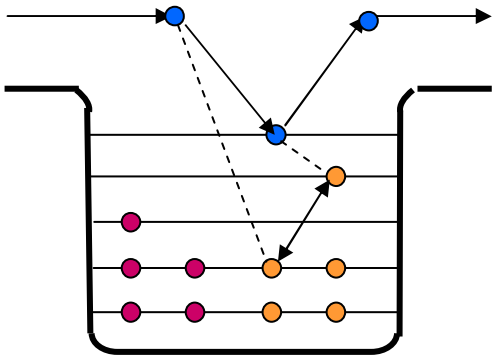

$\Delta t \sim 10^{-12} - 10^{-20}$ s

In a direct scattering, the incident neutron interacts with the average field of the nucleus. The duration of the collision is approximately the time it takes the neutron to cross the nucleus.

In a compound nuclear scattering, the incident neutron loses energy upon colliding with the nucleus and is trapped. After a fairly long interval, enough energy is again concentrated on one neutron to allow it to escape.

Formalities - I

To formally separate the direct and compound nucleu contributions, we assume that we can partition the space of states into two components:

P -- containing the continuum states, such as the n + ^{58}Ni ones, and

Q -- containing the quasi-bound states, such as the ground and excited states of ^{59}Ni (and any other states that we don't want in P).

We define projection operators, P and Q, onto the subspaces with the properties

$$P^\dagger = P \qquad Q^\dagger = Q,$$
$$P^2 = P \qquad Q^2 = Q,$$
$$P + Q = 1$$

We then decompose the wave function into $\Psi = P\Psi + Q\Psi$, where $P\Psi$ is the continuum component and $Q\Psi$ the quasi-bound component of the wave function.

Formalities - II

Using P and Q, we decompose the Schrödinger equation, $(E - H)\,\Psi = 0$, into coupled equations for the two components of the wave function,

$$(E - H_{PP})P\Psi = V_{PQ}Q\Psi$$

and

$$(E - H_{QQ})Q\Psi = V_{QP}P\Psi,$$

where

$$H_{PP} \equiv PH_0P + PVP, \qquad V_{PQ} \equiv PHQ = PVQ, \quad \text{etc.,}$$

and we have assumed that the contributions of the kinetic energy and the target Hamiltonian, both contained in H_0, do not couple the P and Q subspaces.

We can now solve the second equation formally, using an outgoing wave boundary condition, to obtain $Q\Psi$,

$$Q\Psi = (E^{(+)} - H_{QQ})^{-1}V_{QP}P\Psi$$

and substitute in the first of these to obtain an equation for $P\Psi$ alone,

$$(E - H_{PP} - V_{PQ}(E^{(+)} - H_{QQ})^{-1}V_{QP})P\Psi = 0,$$

and which explicitly contains the direct and compound processes we expect.

Formalities - III

However, it will be useful for us to follow a more convoluted path here. We first solve for the continuum component of the wave function $P\Psi$,

$$P\Psi_c = \phi_c^{(+)} + (E^{(+)} - H_{PP})^{-1} V_{PQ} Q\Psi_c,$$

where the wave function $\phi_c^{(+)}$ satisfies the equation

$$(E - H_{PP})\phi_c^{(+)} = 0,$$

with an incoming wave in channel c. When the solution for $P\Psi$ is substituted in the equation for $Q\Psi$, the latter may be rewritten as

$$(E - H_{QQ} - W_{QQ})Q\Psi_c = V_{QP}\phi_c^{(+)},$$

where

$$W_{QQ} \equiv V_{QP}(E^{(+)} - H_{PP})^{-1} V_{PQ}.$$

In the last expression, we may decompose the P-subspace propagator as

$$\frac{1}{E^{(+)} - H_{PP}} = \frac{P.P.}{E - H_{PP}} - i\pi\delta(E - H_{PP})$$

where P.P. is the principal part. The open channels in the P subspace make a negative imaginary contribution to W_{QQ}, leading to poles of the the wave function in the lower half of the complex energy plane.

Formalities - IV

If we solve the equation for the Q - subspace component,

$$(E - H_{QQ} - W_{QQ})Q\Psi_c = V_{QP}\phi_c^{(+)} \quad \Rightarrow \quad Q\Psi_c = (E - H_{QQ} - W_{QQ})^{-1} V_{QP}\phi_c^{(+)},$$

we may substitute this in the solution for the P-subspace component,

$$P\Psi_c = \phi_c^{(+)} + (E^{(+)} - H_{PP})^{-1} V_{PQ} Q\Psi_c,$$

to immediately obtain,

$$P\Psi_c = \phi_c^{(+)} + (E^{(+)} - H_{PP})^{-1} V_{PQ} (E - H_{QQ} - W_{QQ})^{-1} V_{QP}\phi_c^{(+)}.$$

This is a solution for the complete P-subspace wave function in terms of pure continuum component $\phi_c^{(+)}$ and a compound nucleus component. The prompt contribution of V_{PP} to the scattering is not as visible as before – it is contained in the wave function $\phi_c^{(+)}$ and in the P-subspace propagator. The compound nucleus term appears in a modified form, in which passage through the continuum is taken into account by the W_{QQ} term in the Q-subspace propagator.

Low-energy neutron scattering -- resonances

We may now take the expression for the P - subspace wave function,

$$P\Psi_c = \phi_c^{(+)} + (E^{(+)} - H_{PP})^{-1} V_{PQ} (E - H_{QQ} - W_{QQ})^{-1} V_{QP} \phi_c^{(+)},$$

and apply it to s-wave neutron scattering, for which,

$$\psi_0(r) = \frac{i}{2kr}(e^{-ikr} - S_0 e^{ikr}),$$

outside the range of the interaction. (We continue to neglect the spin of the neutron.)

After a bit of work, we can approximate the S-matrix of the P-subspace wave function in a multi-level Breit-Wigner form (among others) as

$$S_{0,ab} = e^{-i(\phi_a + \phi_b)} \left(\delta_{ab} - i \sum_{\mu} \frac{g_{\mu a} g_{\mu b}}{E - \varepsilon_\mu + i\Gamma_\mu / 2} \right),$$

where ϕ_a and ϕ_b are the initial and final channel phase shifts and $g_{\mu c}$ characterizes the coupling of the compound state μ to the continuum channel c, with $\Gamma_\mu = \sum_c g_{\mu c}^2$.

The phase shifts vary slowly with the energy while the resonance sum varies quickly.

Low-energy neutron scattering – cross sections

The cross sections directly related to the elastic S-matrix element are the elastic, absorption and total ones,

$$\sigma_{el} = \frac{\pi}{k^2}\left|S_{0,aa} - 1\right|^2, \qquad \sigma_{abs} = \frac{\pi}{k^2}\left(1 - \left|S_{0,aa}\right|^2\right),$$

and

$$\sigma_{tot} = \sigma_{el} + \sigma_{abs} = \frac{2\pi}{k^2}\left(1 - \mathrm{Re}\, S_{0,aa}\right).$$

The absorption cross section is non-zero when non-elastic channels, such as γ emission or fission, remove flux from the compound nucleus. The cross sections for these take the form

$$\sigma_{ac} = \frac{\pi}{k^2}\left|S_{0,ca}\right|^2.$$

The total flux is conserved,so that

$$\sigma_{abs} = \sum_{c \neq a} \sigma_{ca} \qquad \text{and} \qquad \sigma_{tot} = \sigma_{el} + \sigma_{abs}.$$

The elastic cross section is well described at energies below the resonance region by a hard-sphere cross section of $4\pi R^2$.

Comparison with experiment -- n+^{235}U

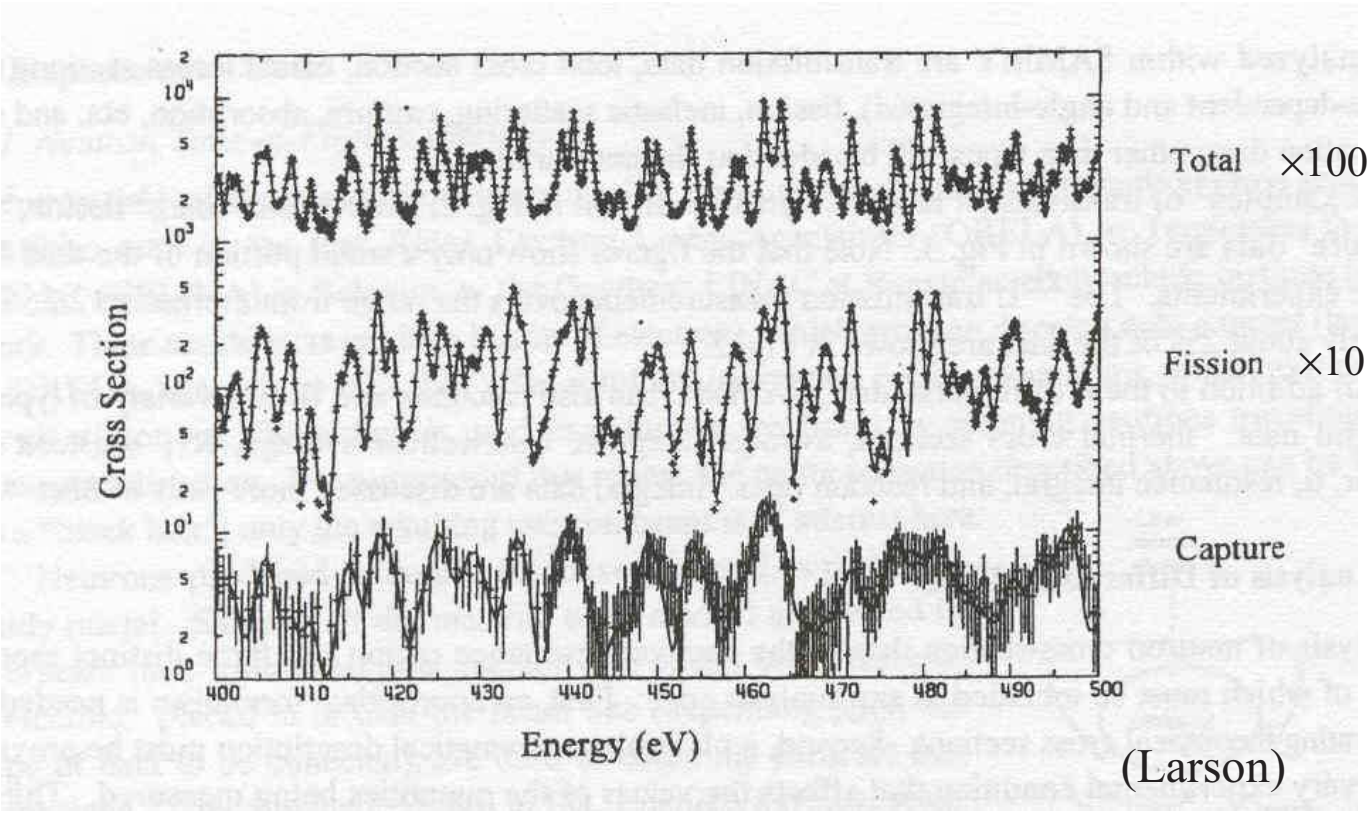

(Larson)

These experimental data for the total, fission and neutron capture cross sections are well described by the superposition of scattering from a potential and reactions through compound nucleus resonances.

The large number of resonances permits a statistical analysis of their properties.

Level statistics

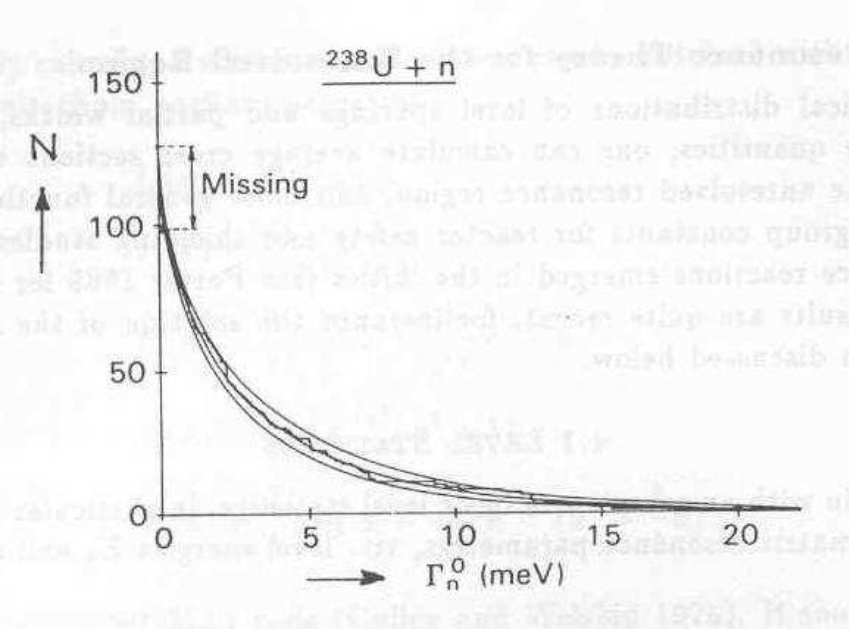

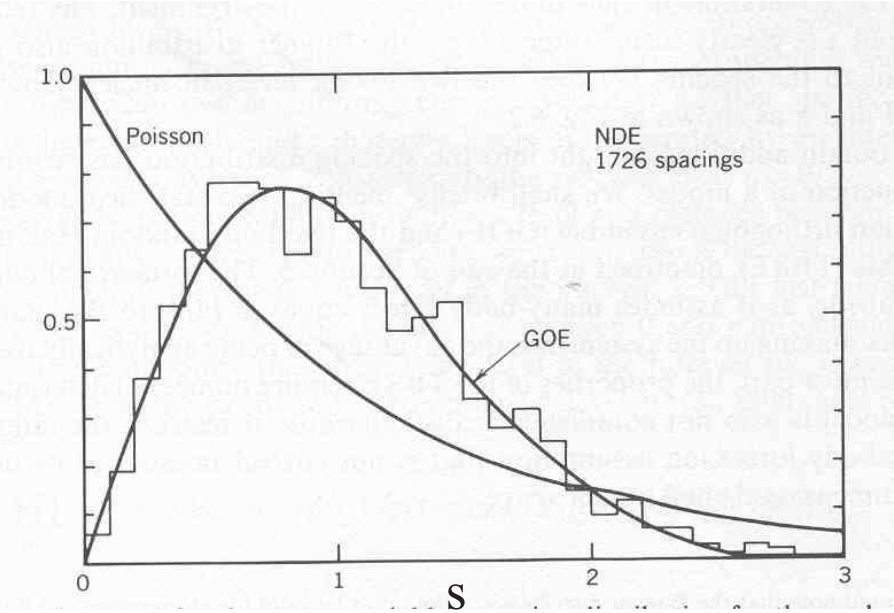

A statistical analysis shows that the reduced neutron partial widths, $\Gamma^0{}_{n\mu} = g^2_{\mu n} / P_\mu$, and the level spacings, $D_\mu = \varepsilon_{\mu+1} - \varepsilon_\mu$, in each partial wave, are distributed as

$$P(x) = \frac{1}{2\sqrt{\pi}} \frac{e^{-x}}{\sqrt{x}}, \qquad x = \Gamma^0{}_n / \left\langle \Gamma^0{}_n \right\rangle \qquad \text{and} \qquad P(s) = 2s\, e^{-s^2}, \qquad s = \frac{\pi}{2} \frac{D}{\langle D \rangle}$$

Porter-Thomas Wigner

These results are consistent with the hypothesis that the matrix elements of V_{PQ}, V_{QP} and V_{QQ} are random variables with Gaussian distributions -- $P(v) = \frac{1}{\sqrt{\pi}} e^{-v^2}$.

From resonances to fluctuations

At low energies, the resonance expression for the S-matrix permits the separation of the direct and compound contributions to cross sections. However, as the energy increases, both the resonance widths and the density of compound nucleus states increase, so that the resonances eventually overlap and can no longer be distinguished. The cross section fluctuates rapidly, as in the figure, but the fluctuations, called Ericson fluctuations, cannot be attributed to individual resonances.

It is in this context that the optical model plays a fundamental role. The objective of the model is to describe just the prompt, direct reactions in a collision. To this end, one defines the optical potential as the potential that furnishes the energy-averaged (short time) scattering amplitudes.

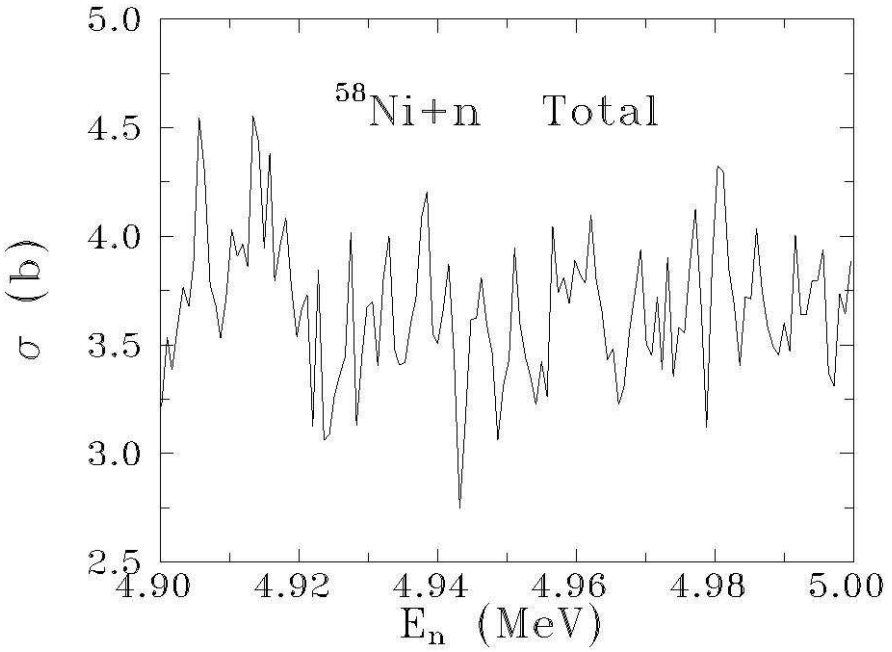

Average amplitudes and cross sections

An energy average of the wave function furnishes a wave function and a scattering amplitude that should describe the prompt part of the scattering. The S-matrix that results is an energy-averaged one. We could write the S-matrix before averaging as

$$\mathsf{S}_l = S_l + S_{l,fluc}, \quad \text{with} \quad \langle S_{l,fluc} \rangle = 0, \quad \text{so that} \quad \langle \mathsf{S}_l \rangle = S_l.$$

The energy-averaged total cross-section is just the optical one,

$$\sigma_{tot,l} = \frac{2\pi}{k^2}\left(1 - \mathrm{Re}\langle \mathsf{S}_l \rangle\right) = \frac{2\pi}{k^2}\left(1 - \mathrm{Re}\, S_l\right),$$

since it is linear in the S-matrix.

However, the energy-averaged elastic and absorption cross sections are

$$\sigma_{el,l} = \frac{\pi}{k^2}\left\langle \left|\mathsf{S}_l - 1\right|^2 \right\rangle = \frac{\pi}{k^2}\left|S_l - 1\right|^2 + \frac{\pi}{k^2}\left\langle \left|S_{l,fluc}\right|^2 \right\rangle$$

and

$$\sigma_{abs,l} = \frac{\pi}{k^2}\left\langle 1 - \left|\mathsf{S}_l\right|^2 \right\rangle = \frac{\pi}{k^2}\left(1 - \left|S_l\right|^2\right) - \frac{\pi}{k^2}\left\langle \left|S_{l,fluc}\right|^2 \right\rangle.$$

Only the total optical cross section may be compared with the experimental one.

Energy averaging and the optical model

The energy average of the P-subspace wave function yields the optical wave function and scattering amplitude, which describe the fast contribution to the scattering. After rewriting the expression for the wave function in the form of an equation, we obtain an expression for the optical potential.

The energy average of the P-subspace wave function may be written directly,

$$\left\langle P\Psi_c \right\rangle = \phi_c^{(+)} + (E^{(+)} - H_{PP})^{-1} V_{PQ} \left\langle 1/e_{QQ} \right\rangle V_{QP} \phi_c^{(+)}.$$

since the only rapidly varying quantity in the wave function is

$$e_{QQ} = E - H_{QQ} - W_{QQ}.$$

By multiplying by (E-H_{PP}) as well as solving formally for $\phi_c^{(+)}$ and substituting, we can write a Schrödinger-like equation for $\langle P\Psi_c \rangle$.

,

$$\left(E - H_{PP} - V_{PQ} \frac{1}{\left\langle 1/e_{QQ} \right\rangle^{-1} + W_{QQ}} V_{QP} \right) \left\langle P\Psi_c \right\rangle = 0.$$

The optical potential, which has both real and imaginary parts, is then

$$U_{opt} = V_{PP} + V_{PQ} \frac{1}{\left\langle 1/e_{QQ} \right\rangle^{-1} + W_{QQ}} V_{QP}$$

Performing the energy average

To conclude the derivation of the optical potential, we must calculate $\langle 1/e_{QQ}\rangle$. Although there are many ways to perform the average, the simplest is to average over a normalized Lorentzian density,

$$\left\langle 1/e_{QQ}\right\rangle = \int dE_0 \, \frac{\rho(E,E_0)}{E_0 - H_{QQ} - W_{QQ}}$$

where

$$\rho(E,E_0) = \frac{\Delta}{2\pi}\frac{1}{(E-E_0)^2 + \Delta^2/4}.$$

Assuming that $1/e_{QQ}$ has no poles in the upper half of the complex E plane (causality), we can perform the integral by closing the contour in the UHP to find

$$\left\langle 1/e_{QQ}\right\rangle = (E + i\Delta/2 - H_{QQ} - W_{QQ})^{-1}$$

so that

$$U_{opt} = V_{PP} + V_{PQ}\frac{1}{E - H_{QQ} + i\Delta/2}V_{QP}$$

The optical potential is energy-dependent, non-local and complex. Its imaginary part is negative, resulting in a potential that is absorptive. The absorption accounts for the flux that is lost to the Q-subspace.

Low-energy neutron scattering – optical potential

One finds for the low-energy neutron s-wave S-matrix element $S_0 = e^{-2ik\rho}$, where ρ is a complex scattering length. $R = |\rho|$ is called the scattering radius.

The resulting elastic cross section tends to a constant as the energy tends to zero, while the absorption and total cross sections diverge at small energy as *1/k*.

We have, as $k \to 0$,

$$\sigma_{el} = 4\pi \frac{d\sigma}{d\Omega} \to 4\pi R^2,$$

$$\sigma_{abs} \to -\frac{4\pi}{k} \operatorname{Im} \rho \left(1 + 2k \operatorname{Im} \rho\right),$$

and

$$\sigma_{tot} = \sigma_{el} + \sigma_{abs}.$$

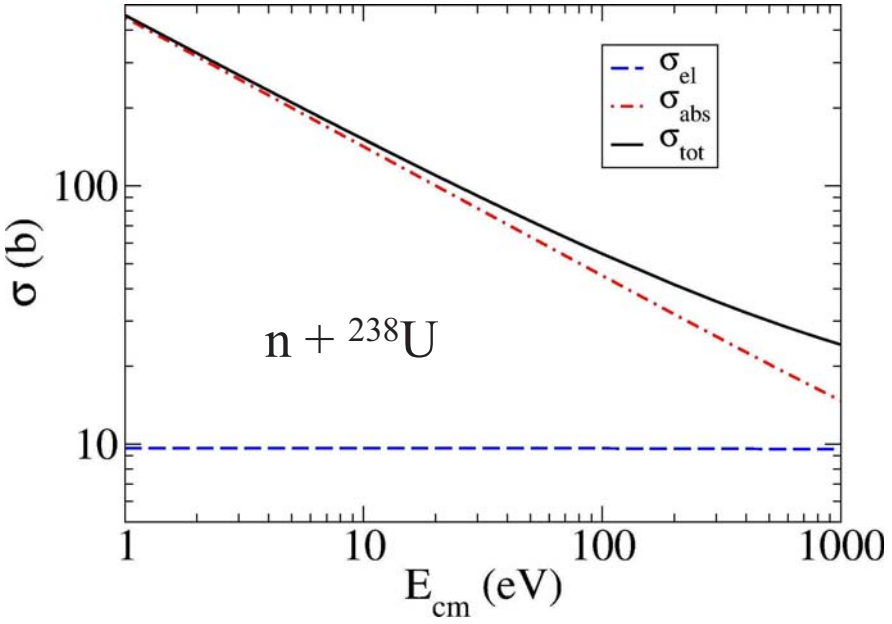

Comparison with experiment

We recall that, being linear in the scattering amplitude, the total optical cross section may be compare to the energy-averaged experimental one. We see that reasonable agreement with the data is possible here.

We also verified that the partial wave contributions to the energy-averaged elastic cross section,

$$\sigma^{j}_{l,el} = \frac{\pi}{k^2}\left|S^{j}_{l} - 1\right|^2 + \frac{\pi}{k^2}\left\langle \left|S^{j}_{l,fluc}\right|^2 \right\rangle$$

exceed the shape elastic (optical) ones due to contributions from fluctuations. We observe that the fluctuation contributions are negligible only at higher energies.

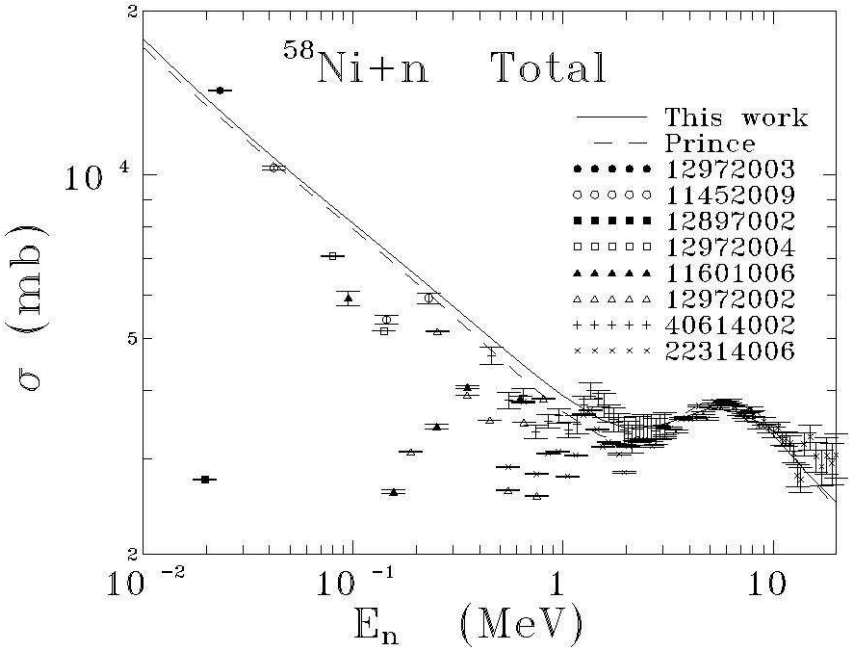

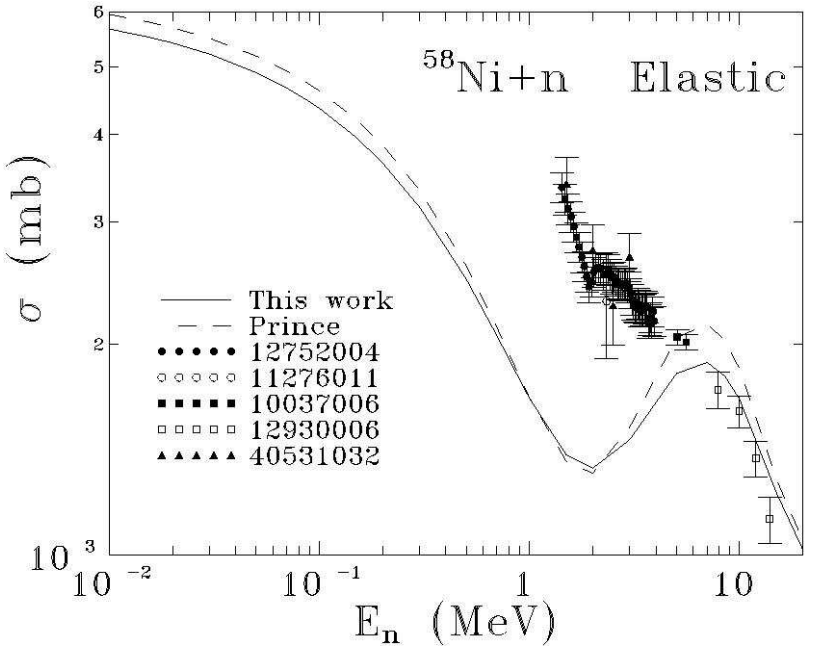

Higher partial waves

The angular distribution for a pure s-wave is obviously constant. As the energy increases, more partial waves participate in the scattering and the angular distribution becomes more forward peaked.

The highest partial wave contributing to the scattering may be crudely estimated as $l_{max} \approx kR$. For n+^{238}U at an energy of 1 MeV, this gives $l_{max} \approx 1.6$.

An important auxiliary quantity determined in an optical model calculation is the transmission coefficient, $T_l = 1 - |S_l|^2$, which is used to calculate the fluctuating contribution to the cross sections. The transmission coefficient measures the fraction of flux that is absorbed from each partial wave.

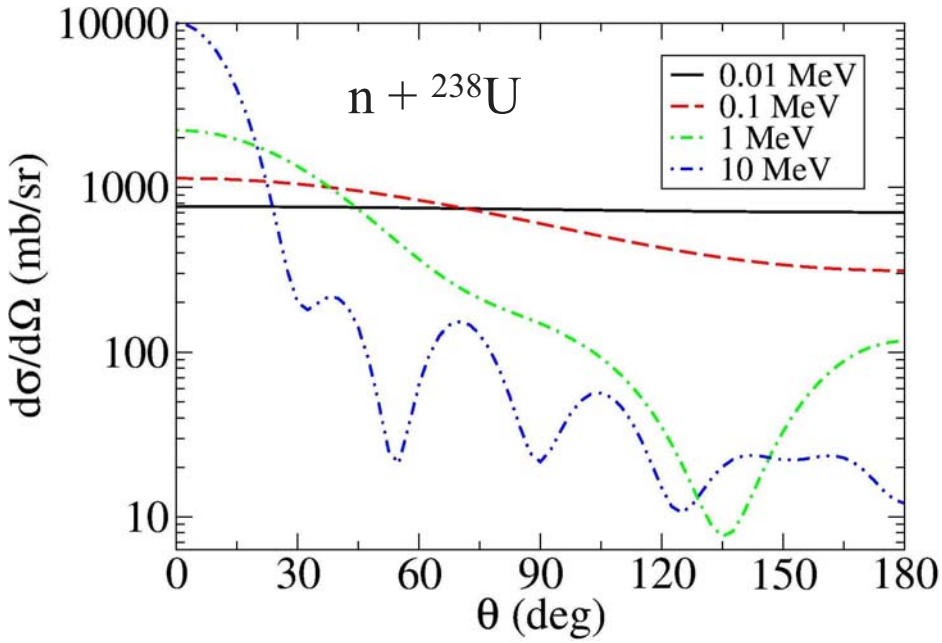

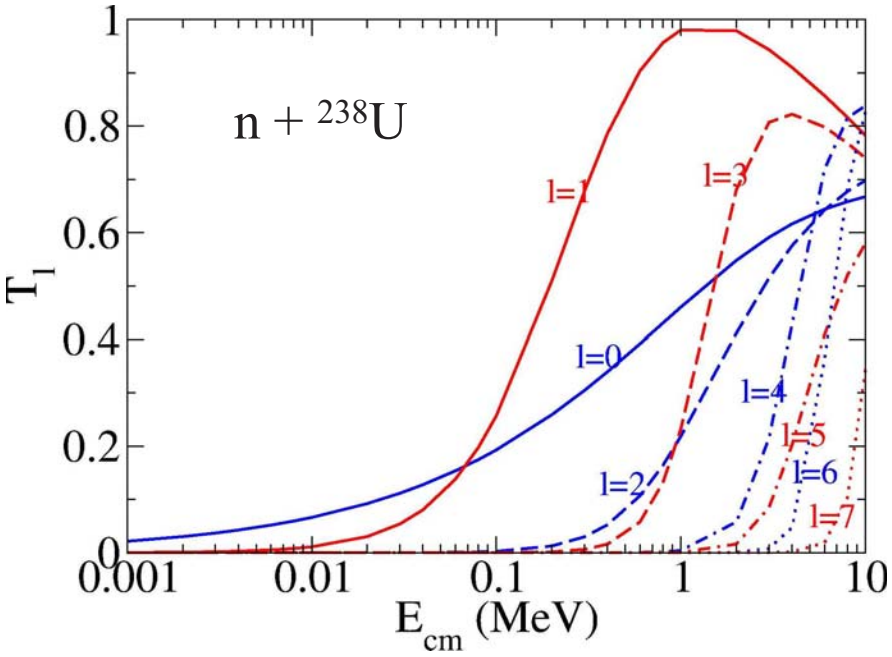

Inelastic scattering

The single-channel optical model describes the scattering in the elastic channel alone. It is often called the spherical optical model because, in it, the target may be considered to be spherically symmetric, since its structure is never introduced.

Inelastic scattering, in the case of the inert projectiles that we are considering (n, p, γ, d, etc.), leaves the target in an excited state and diminishes the asymptotic kinetic energy of the projectile. To describe it, we must introduce at least the basic characteristics of the ground and excited states of the target. The states that are most strongly excited in collisions are those that involve collective movement.

Vibrations:

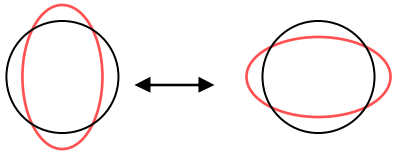

Rotations:

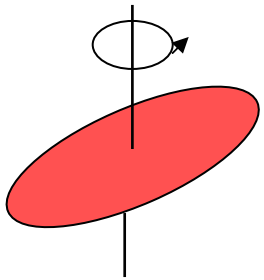

Direct excitation of rotational and vibrational modes is usually calculated using the coupled channels method. This is an extension of the optical model formalism that treats the ground and excited states on an equal footing.

Comparison with experiment

Inelastic cross sections are dominated by the contribution from the compound nucleus at low energies, as seen here for the first excited states of ^{58}Ni and ^{238}U.

The two calculations of the ^{58}Ni inelastic cross section use the same value of β_2=0.2, yet yield cross sections that differ by almost a factor of two due to differences in the optical potentials.

The cross section for excitation of the rotational state in ^{238}U is 5 to 10 times greater than that of the vibrational state in ^{58}Ni, mainly due to the factor of 30 difference in their excitation energies.

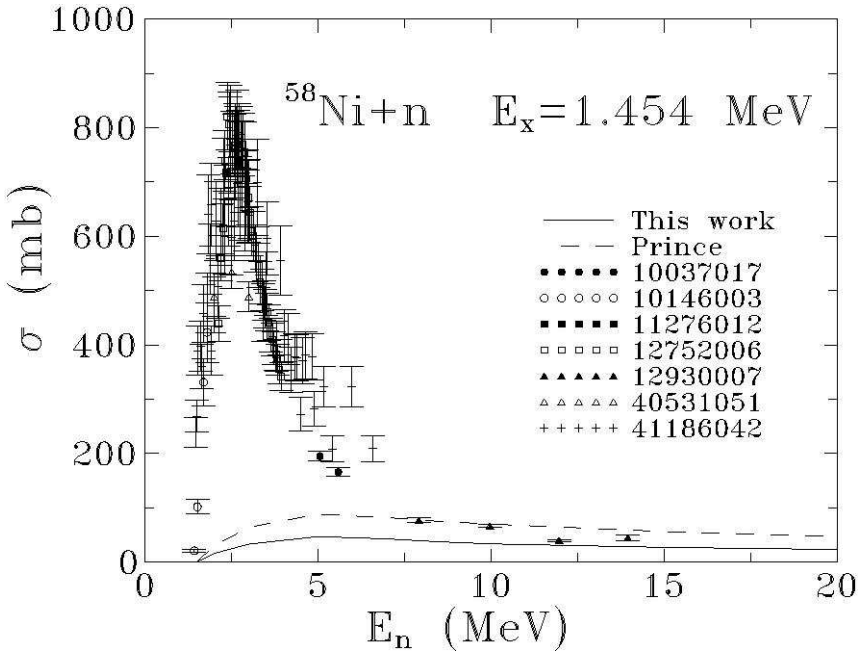

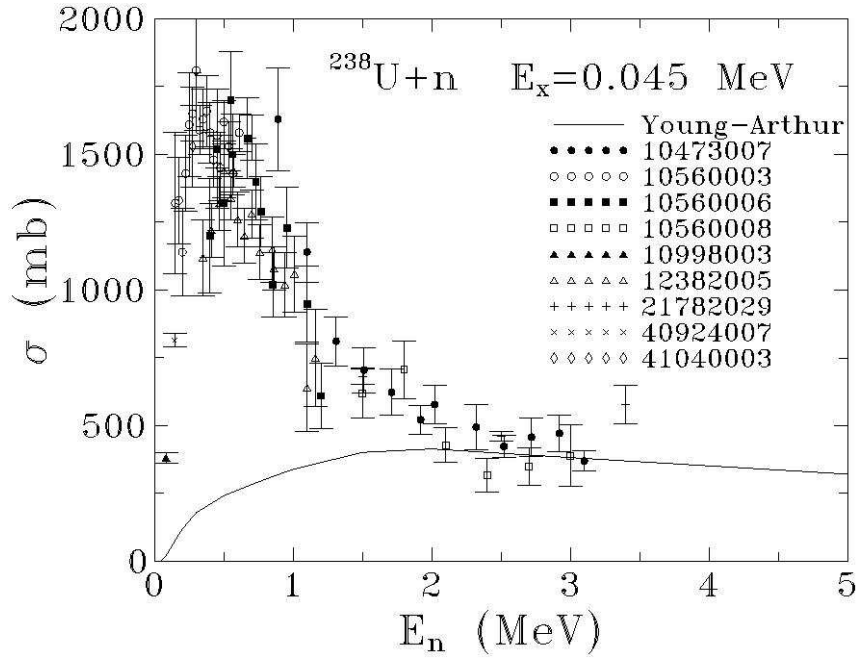

Energy averaging and the compound nucleus

We decomposed the S-matrix in channel *a* and partial wave *l*, before averaging over energy, as

$$\mathsf{S}_{al} = S_{al} + S_{al,fluc}, \quad \text{with} \quad \langle S_{al,fluc} \rangle = 0, \quad \text{so that} \quad \langle \mathsf{S}_{al} \rangle = S_{al}.$$

The elastic cross section that resulted is the sum of an optical contribution and a compound nucleus one,

$$\sigma_{aa,l} = \frac{\pi}{k^2} \langle |\mathsf{S}_{al} - 1|^2 \rangle = \frac{\pi}{k^2} |S_{al} - 1|^2 + \frac{\pi}{k^2} \langle |S_{al,fluc}|^2 \rangle.$$

If we neglect direct coupling between channels, the cross section for a reaction from channel a to channel *b* will consist of just the compound nucleus contribution,

$$\sigma_{ab,l} = \frac{\pi}{k^2} \langle S_{bl,fluc}{}^{*} S_{al,fluc} \rangle.$$

The compound nucleus cross sections can be calculated, if we substitute the energy average by an average over the random interaction matrix elements used to construct the resonance sum. (Weidenmüller et al.)

The Bohr hypothesis

The average cross section has the form

$$\sigma_{ab} = w_{ab}\sigma_a^C \frac{\Gamma_b^C}{\Gamma^C},$$

where σ_a^C is the cross section for compound nucleus formation from channel a, Γ_b^C is the partial width for decaying into channel b, with the total width being

$$\Gamma^C = \sum_b \Gamma_b^C .$$

The width fluctuation factor w_{ab} varies between 2 and 3 for the elastic channel. For other channels, it is close to one, except at very low energies. If we neglect it here, we satisfy the Bohr hypothesis, which states that the formation and decay of the compound nucleus are independent processes. This was tested experimentally by Goshal in 1950.

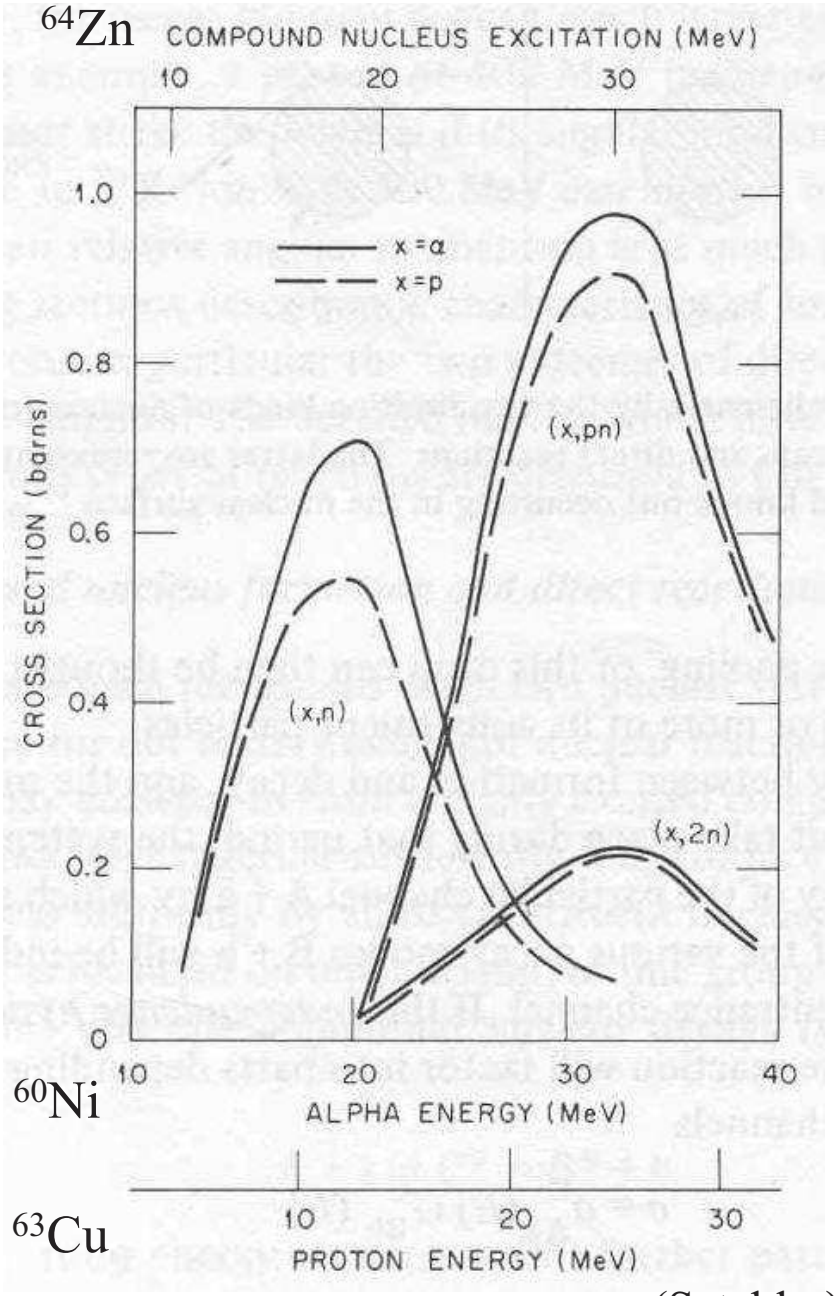

(Satchler)

Angular distributions

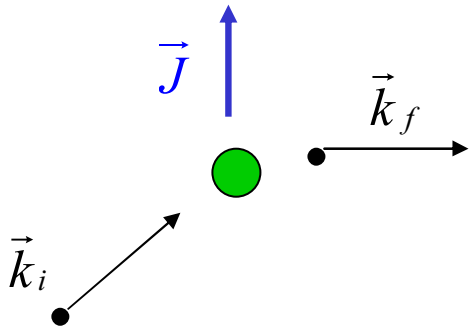

Due to the independence of the formation and decay of the compound nucleus, the decaying nucleus does not 'remember' the direction of the incident projectile. It does 'remember' the conserved angular momentum, however. If the angular momentum is zero, the decay is isotropic. Otherwise, it tends to be restricted to the reaction plane. The angular distribution is always symmetric about 90°.

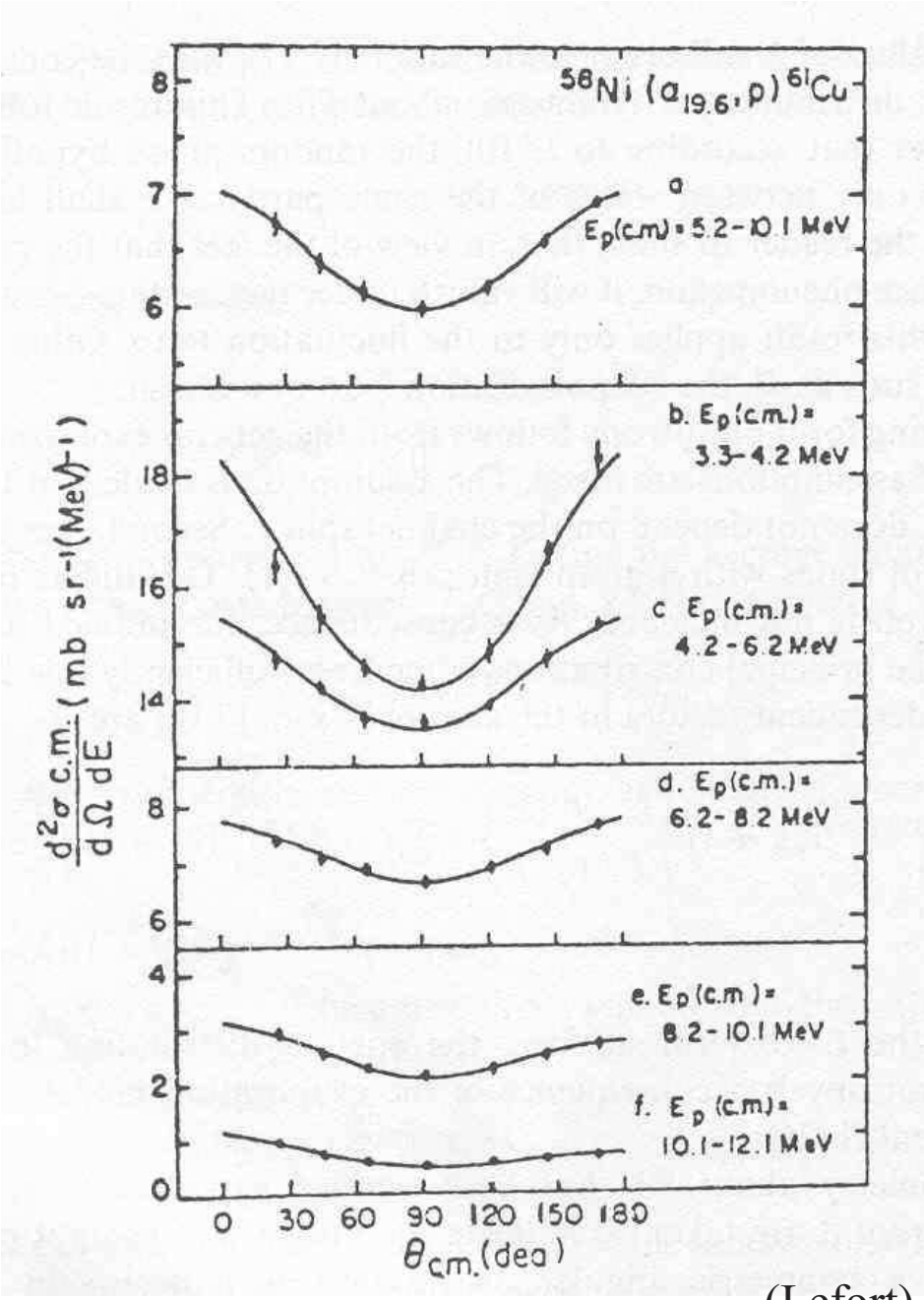

(Lefort)

Level densities and emission spectra

In regions of unresolved levels,

$$2\pi\rho_C(E)\Gamma_b^C(\varepsilon_b) = (2s_b+1)k_b^2\sigma_b^C(\varepsilon_b)N_b(\varepsilon_b).$$

with $N_b(\varepsilon_b) = \rho(E-\varepsilon_b-B_b)\Delta\varepsilon_b.$

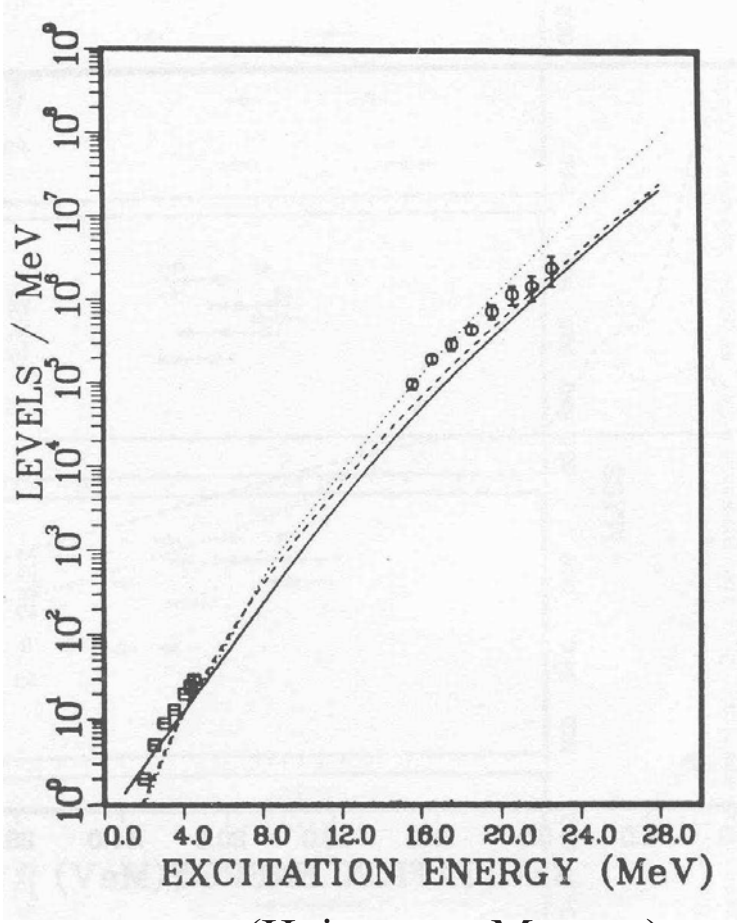

(Huizenga e Moretto)

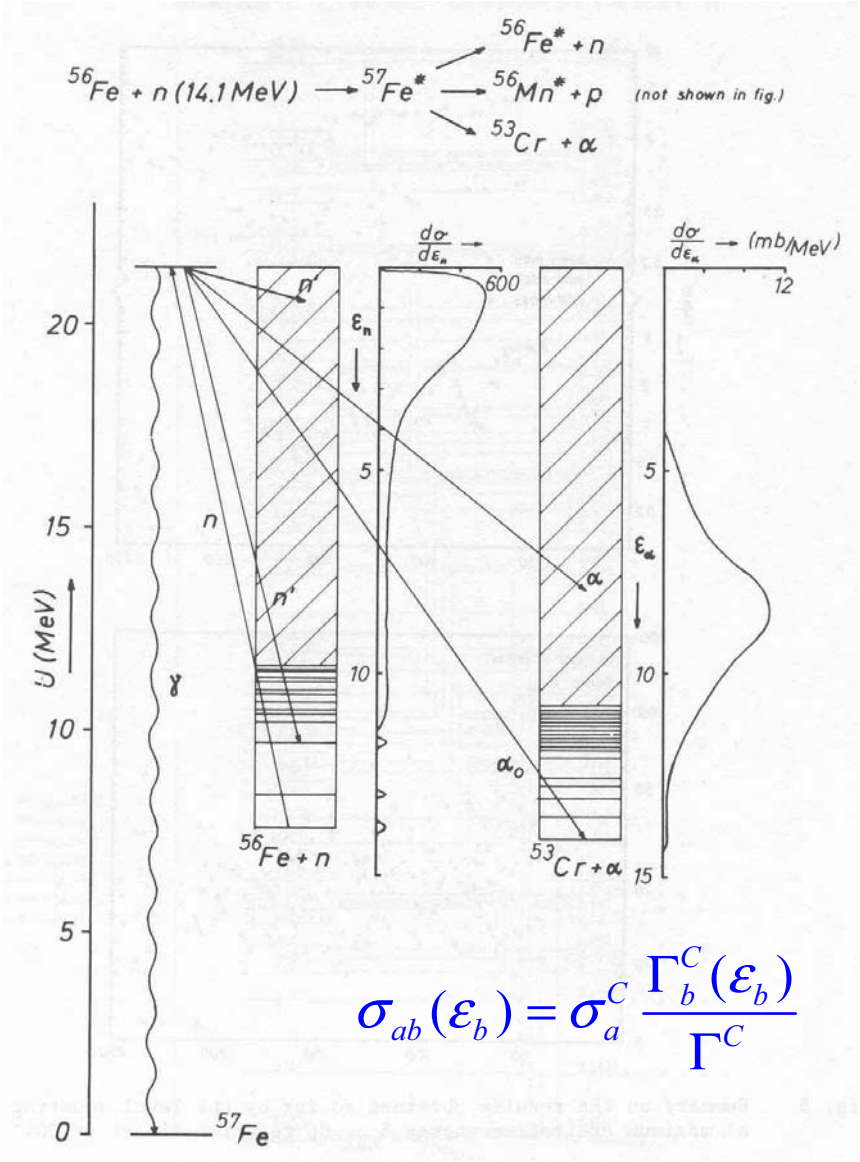

$$\sigma_{ab}(\varepsilon_b) = \sigma_a^C \frac{\Gamma_b^C(\varepsilon_b)}{\Gamma^C}$$

(Vonach)

Excitation function of a level

For a single level or a group of levels, we have

$$2\pi\rho_C(E)\Gamma_b^C(\varepsilon_b) = (2s_b+1)k_b^2\sigma_b^C(\varepsilon_b)N_b(\varepsilon_b) \quad \text{and} \quad \sigma_{ab}(\varepsilon_b) = \sigma_a^C\frac{\Gamma_b^C(\varepsilon_b)}{\Gamma^C}.$$

The cross section just above threshold increases with the available energy, quickly in the case of neutrons, but more slowly in the case of charged particles.

However, the number of levels contributing to the total width Γ^C increases exponentially with the energy, in accord with the density of states. The compound nucleus cross section for the level(s) thus reaches a maximum and then falls back to zero exponentially.

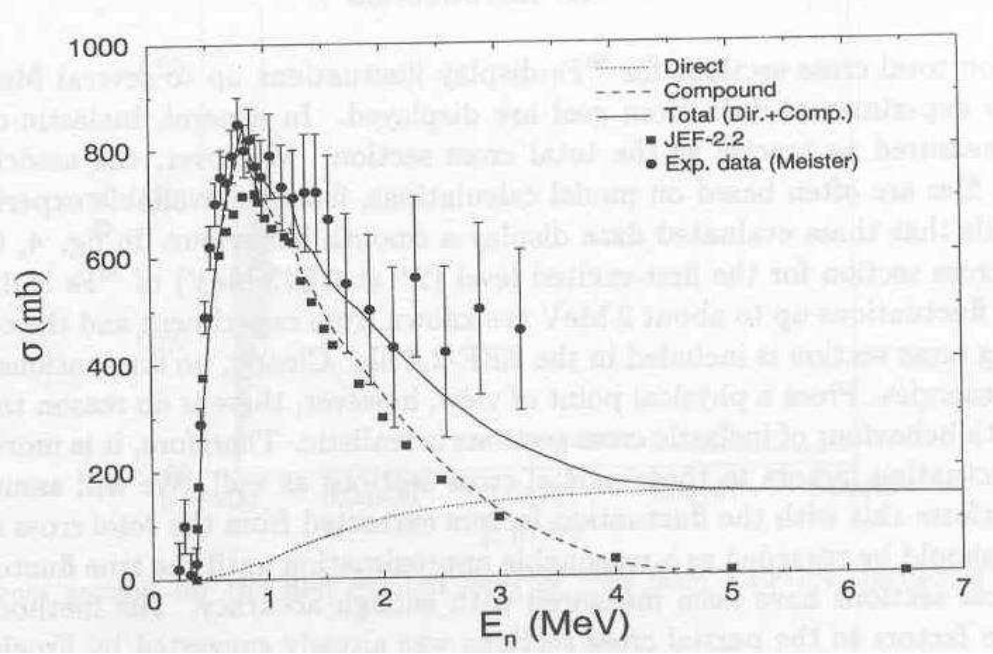

$n+^{110}Pd \rightarrow n' + ^{110}Pd^*(E_x=0.374\ MeV, 2+)$

(Koning)

Competition and multiple emission

All open channels compete for emission from the compound nucleus. However, γ emission is a much weaker (much slower) process than particle emission. Charged particle emission tends to be suppresses relative to neutron emission because of the Coulomb barrier.

At sufficiently high energies, a compound nucleus can emit more than one particle. This is treated as sequential emission and can be incorporated in the model by keeping track of the distribution of residual nuclei. Calculations at high energy can be lengthy, due to the many open channels.

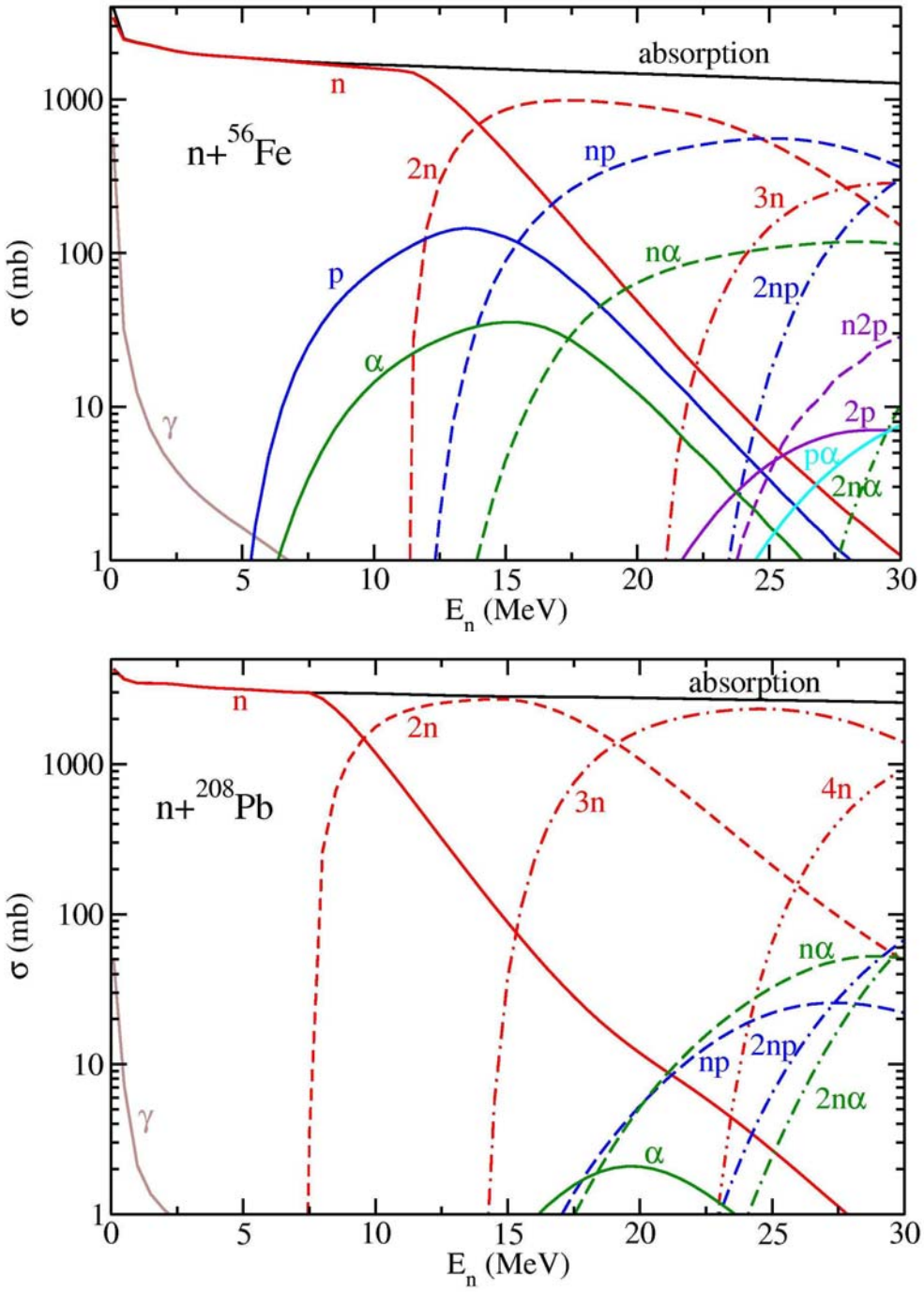

Preequilibrium emission

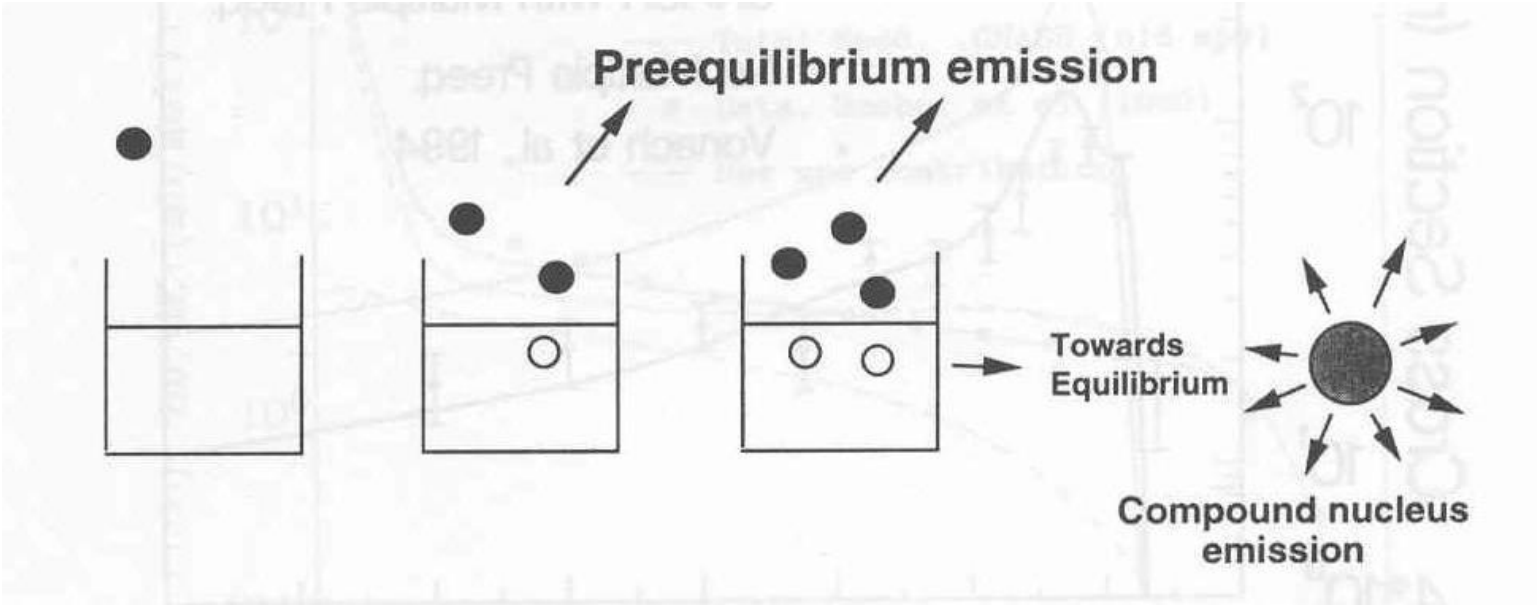

Compound nucleus models assume that the nucleus reaches an equilibrium (all states are equally probable) before emission occurs. Physically, the equilibration process proceeds through a series of nucleon-nucleon reactions. As the incident energy increases, it becomes more and more likely that one of the nucleons still retains a large fraction of the incident energy after the first one or two collisions, which favors its emission from a preequilibrium configuration.

Multistep compound (MSC) emission

To analyzed preequilibrium compound processes, we partition the subspace of states Q into a series of subspaces containg configurations of increasing complexity,

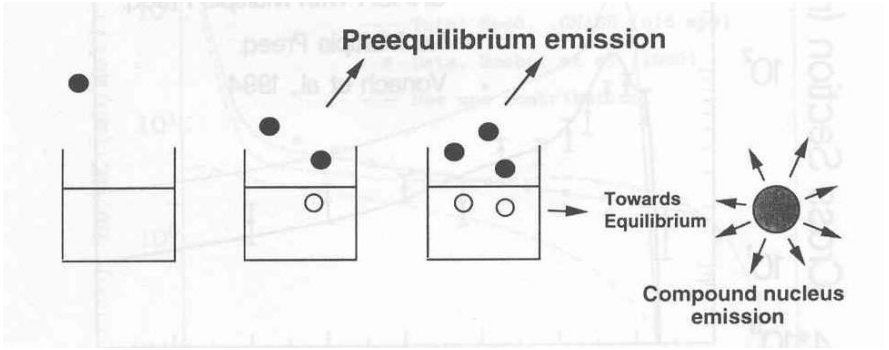

$$Q = Q_1 + Q_2 + Q_3 + \ldots + CN$$

2p-1h 3p-2h 4p-3h

One now takes into account transitions between the subspaces Q_n as well as emission from each of them,

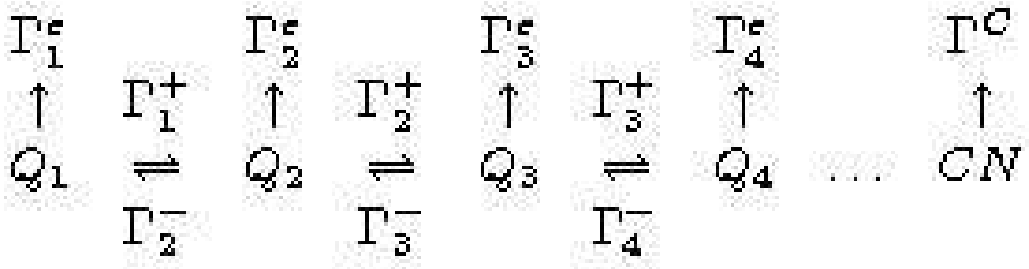

The transition and emission widths can be calculated using the model of random matrix elements or using simple physical arguments. Essential in both cases is the hypothesis that the states in each subspace are in equilibrium.

Multistep compound (MSC) emission - calculations

Multistep compound cross sections are calculated by solving the set of coupled linear equations that describe the distribution of the flux over the different subspaces.

Calculations show that the principal contributions to the cross sections come from the simplest configurations (n=1 or 2) and from the complex configurations that correspond to equilibrium.

When the emission widths are small compared to the internal transition widths, only the equilibrium configuration contributes and a simple expression for the cross section, similar to the compound nucleus one, is recovered.

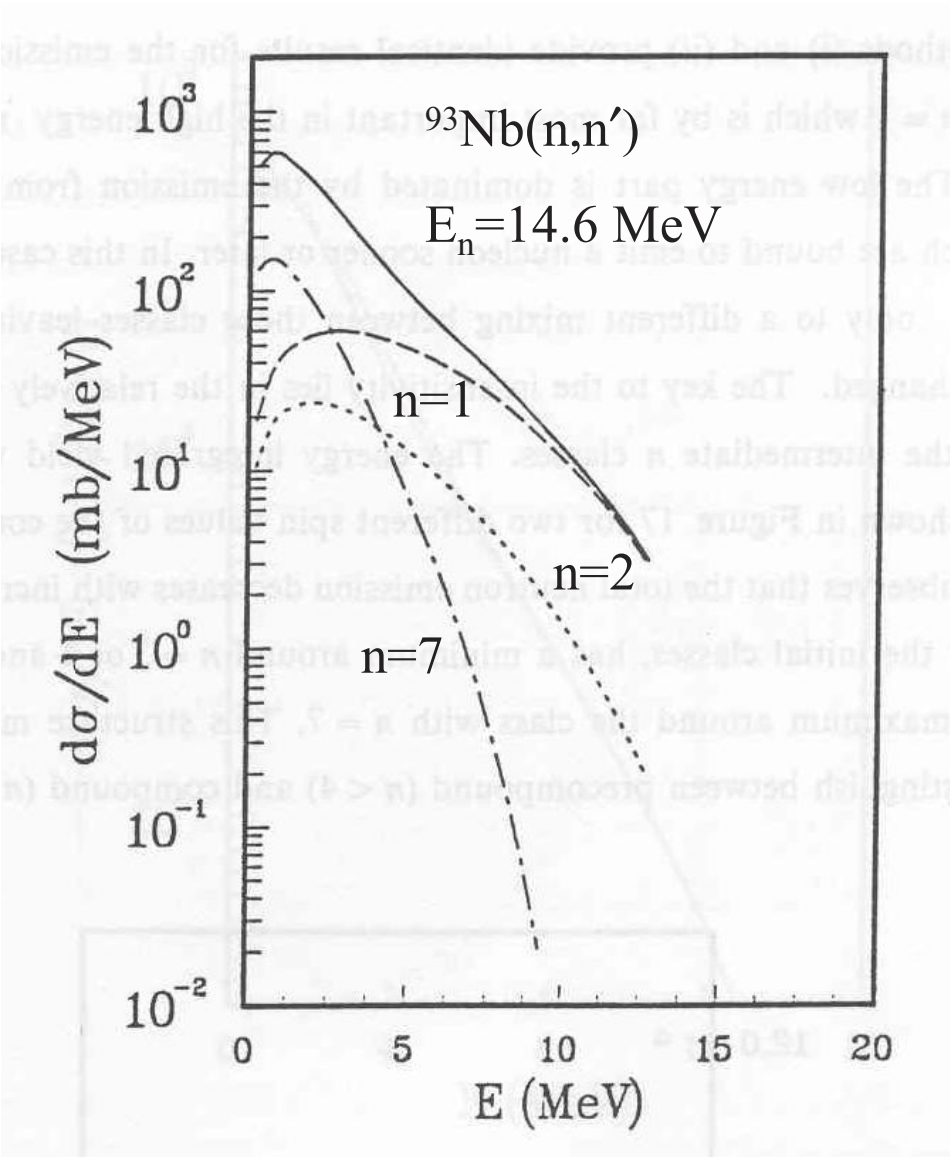

(Herman)

Multistep direct (MSD) emission

To analyzed direct preequilibrium processes, we partition the subspace of states P into a series of subspaces containg configurations of increasing complexity,

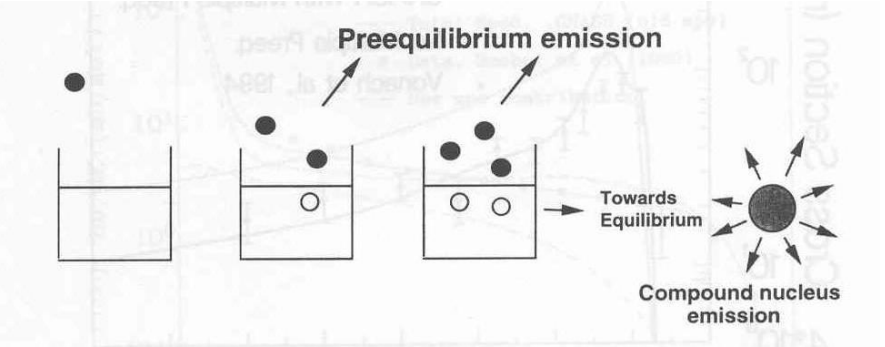

$$P = P_1 + P_2 + P_3 + \ldots + CN$$

1p-1h 2p-2h 3p-3h

Here one takes into account only the transitions between the subspaces $P_{n.}$ The incident particle maintains its identity. No hypothesis is necessary concerning equilibrium among the states with the same number of particles and holes.

The process is described using a direct extension of the DWBA treatment of weakly excited levels. The differential cross section is written as an incoherent sum of one-step and multistep terms,

$$\frac{d^2\sigma_{b\leftarrow a}(E,\Omega\leftarrow E_0,\Omega_0)}{dEd\Omega} = \sum_{n=1}^{\infty}\frac{d^2\sigma^{(n)}_{b\leftarrow a}(E,\Omega\leftarrow E_0,\Omega_0)}{dEd\Omega}.$$

Multistep direct reactions

The one-step cross section is calculated by summing the DWBA cross sections to the particle-hole states μ, weighted by a broadened density of states $\hat{\rho}_{11}$,

$$\frac{d^2\sigma^{(1)}_{b\leftarrow a}(E,\Omega\leftarrow E_0,\Omega_0)}{dEd\Omega}=\sum_{\mu}\hat{\rho}_{11}(E_0-E,\mu)\frac{d^2\sigma^{DWBA}_{b\leftarrow a,\mu}(E,\Omega\leftarrow E_0,\Omega_0)}{d\Omega}.$$

Since the low-energy collective states are, to a large degree, 1p-1h states, they can be considered a part of the first step of the multistep direct cascade.

The n-step cross section is then usually calculated by convoluting the (n-1)-step cross section and summing over all intermediate configurations,

$$\frac{d^2\sigma^{(n)}_{b\leftarrow a}(E,\Omega\leftarrow E_0,\Omega_0)}{dEd\Omega}=\frac{m}{(2\pi\hbar)^2}\sum_{c}\int E'dE'd\Omega'\frac{d^2\sigma^{(1)}_{b\leftarrow c}(E,\Omega\leftarrow E',\Omega')}{dEd\Omega}$$
$$\times\frac{d^2\sigma^{(n'-1)}_{c\leftarrow a}(E',\Omega'\leftarrow E_0,\Omega_0)}{dE'd\Omega'}.$$

At the moment, this type of calculation has not been taken beyond the second step.

Multistep direct-multistep compound calculations

Multistep compound angular distributions are symmetric about 90°. Multistep direct ones are smooth but forward peaked. The one-step process dominates the angular distribution at forward angles and low excitation energies, while the higher order processes become more important at backward angles and at larger energy excitation energies.

Compound and multistep compound reactions make an important contribution to particle spectra to energies of about 15 MeV. At higher outgoing energies, collective excitations and multistep direct processes dominate nucleon-induced reactions. This is consistent with the idea of the gradual slowing down of the incident nucleon through multiple nucleon-nucleon collisions.

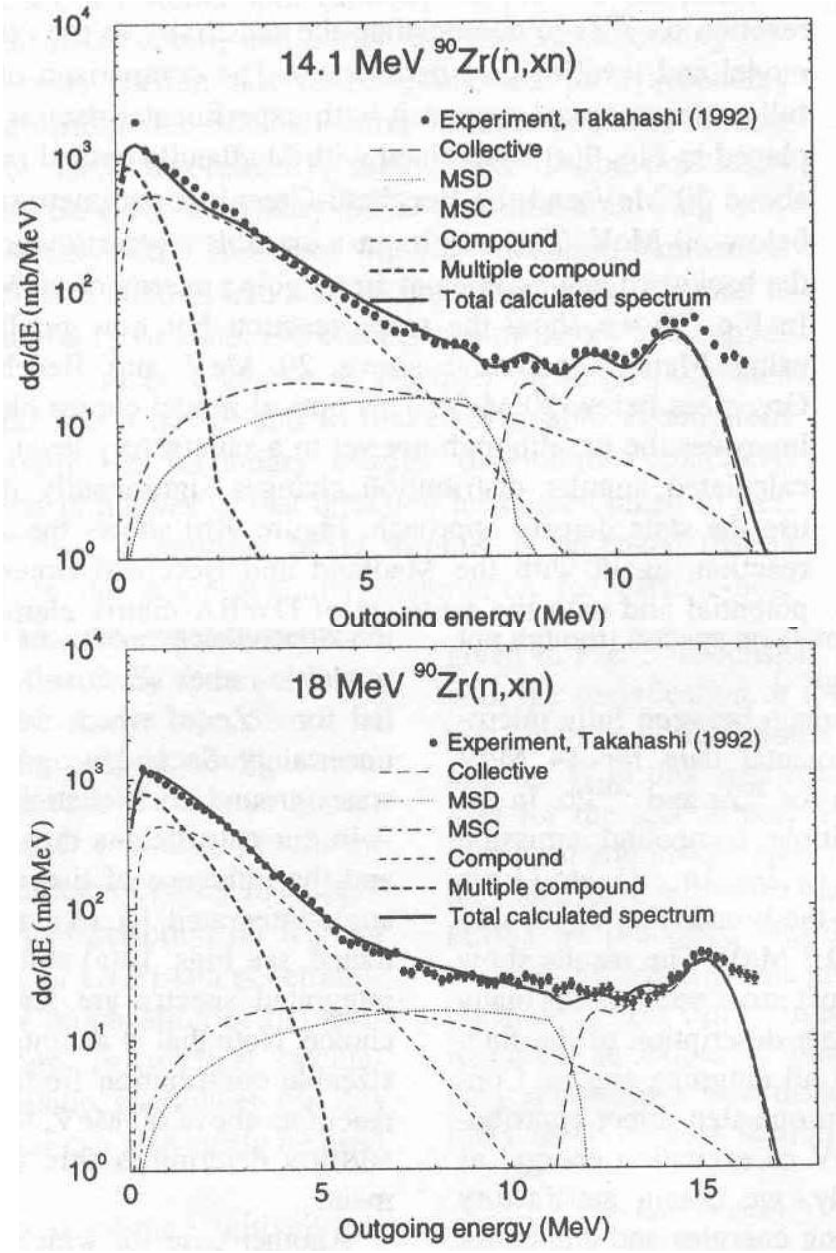

(Koning and Chadwick)

‘Classical’ preequilibrium models

Early (1960’s and 1970’s) preequilibrium models, the exciton and hybrid models, do not distinguish between compound nucleus and continuum states. They include both in a formalism similar to that of the multi-step compound model. The principal differences between the multistep compound model and the earlier ones are:

• the densities of states – only bound states are included in the multistep compound model,

• the emission widths, which require an interaction in the multistep compound model. In the ‘classical’ models, they are obtained directly from the cross sections or transmission coefficients, as in the compound nucleus model.

Although suspect in terms of theoretical rigor, these models are quite succcessful in describing experimental cross sections. Because of their ease of use, when compared to a multistep direct-multistep compound calculation, they are still very popular today.

Mixing in 'classical' preequilibrium models

In the exciton and hybrid models, one assumes that the states with the same number of particles and holes (3p-2h, for example) are in equilibrium. This allows the calculation of transition rates between configurations with different numbers of particles and holes in terms of the densities of states of the configurations:

$\lambda^{+/-}$ - transition rates for increasing /decreasing the number of particles and holes;

λ^{0} - rate of transitions between states with same number of particles and holes – This is essentially the equilibration rate between these states.

Transition rates for n + ^{40}Ca @ 25 MeV (black) and 100 MeV(blue):

$\lambda^{0} << \lambda^{+}$

In the initial stages of the reaction (small number of particles and holes).

No equilibration !

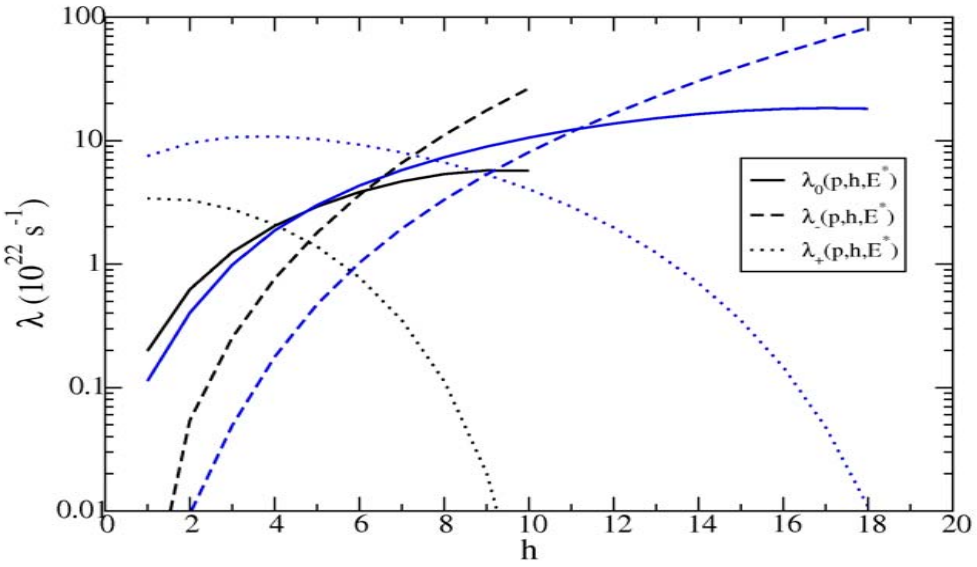

(Hybrid) Monte Carlo simulation

Without the equilibrium hypothesis, the number of equations for the occupation probabilities and emissions becomes immense: for n + ^{40}Ca @ 100 MeV, about 20 equations become on the order of 10^6 equations.

A solution – use a Monte Carlo method to solve the master equation, taking into taking into account
1) each particle or hole, until it no longer has sufficient energy to 'escape';
2) all two-particle interactions.

The blue exciton model result is obtained when the two-body interactions that maintains the number of particles and holes is a 33 times larger than the others.

The black and red results are obtained when these transitions are the same as the others or when they are not included at all.

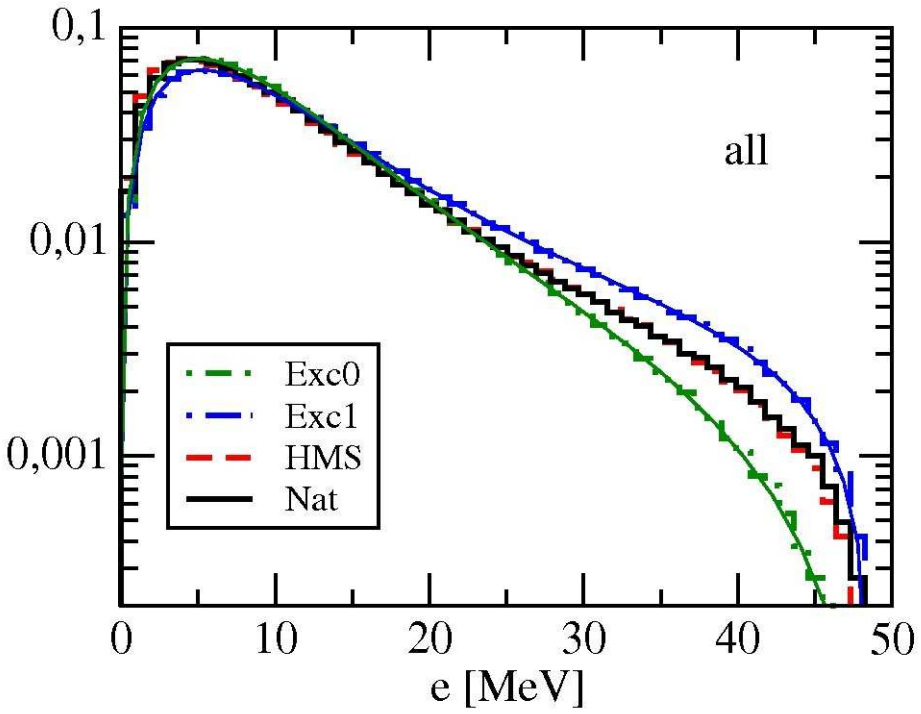

Summary

At low incident energies, nucleon-induced reactions occur on two distinct time scales. Direct reactions, in which the incident particle remains in the continuum, occur quickly. Compound nucleus reactions, in which the projectile is trapped in a quasi-bound state, occur much more slowly.

The corresponding differential cross sections are consistent with their time scales: direct reactions tend to be forward peaked while compound nucleus ones are symmetric about 90°.

Preequilibrium processes corresponding to intermediate time scales arise and become ever more important as the incident energy increases.